Application of the CAB Evaluation of Thermal Scattering Law for Heavy Water to ZED-2 Critical Benchmarks at Room Temperature

D. Roubtsov, J.C. Chow

Canadian Nuclear Laboratories, Chalk River, ON K0J 1J0, Canada

J.I. Márquez Damián, J.R. Granada

Neutron Physics Department and Instituto Balseiro, Centro Atómico Bariloche, Argentina

Abstract

To improve the evaluations in thermal scattering sub-libraries, a set of thermal neutron scattering cross sections (scattering kernels) was developed recently at Centro Atómico Bariloche (CAB) for deuterium and oxygen bound in liquid heavy water, and made available in the ENDF-6 format. These libraries are based on a combination of results of molecular dynamics (MD) simulations and recent experimental data and, when used, result in an improvement of calculations of observables of single neutron scattering experiments, compared to results based on previous evaluations.

In this work, we provide additional details on the CAB evaluation of heavy water at room temperature and discuss the important integral characteristics of neutron scattering kernels, such as the cross sections, average scattering cosine, and average secondary energy. Then, the new set of thermal scattering kernels is applied in modelling criticality of the ZED-2 reactor, and the international benchmarks LEU-MET-THERM-003 (ICSBEP handbook) and ZED2-HWR-EXP-001 (IRPhEP handbook) are analyzed in detail. The differences in the estimates of criticality due to changes in the $S(\alpha, \beta)$ data from the refer-

Email addresses: dan.roubtsov@cnl.ca (D. Roubtsov), marquezj@cab.cnea.gov.ar (J.I. Márquez Damián)

ence one (ENDF/B-VII) to the CAB evaluation are 100 - 200 pcm; they are comparable but smaller than the ZED-2 benchmark uncertainties ($\approx \pm 300$ pcm). Changing the reference evaluation of ^{16}O to the recently developed one from the CIELO project (WPEC subgroup 40) results in a decrease of criticality by ~ 100 pcm. Using different combinations of the improved nuclear data for deuterium, oxygen, and the CAB TSL model, we obtain biases up to 300 - 400 pcm in the estimates of criticality of the selected ZED-2 benchmarks. Application of the new evaluations for ^{235}U and ^{238}U from the CIELO project improves the estimates of k_{eff} by decreasing the bias by ~ 100 pcm that indicates a need for further investigations of the ZED-2 critical assemblies.

1. Introduction

In nuclear science and engineering, nuclear criticality calculations are the solution of an eigenvalue problem associated with systems containing fissile materials near critical condition. The problem solved is an *associated critical reactor* (Henry, 1975), which is expressed as the following linear Boltzmann equation for the system with void (vacuum) boundary conditions:

$$
\begin{aligned}
\left(\hat{\Omega} \cdot \vec{\nabla} + \Sigma_{\mathrm{tot}}(E)\right)&\psi(\vec{r}, E, \hat{\Omega}) = \\
\int_0^\infty \mathrm{d}E^* &\int_{4\pi} \mathrm{d}\hat{\Omega}^* \, \Sigma_{\mathrm{s}}(E^*, \hat{\Omega}^* \to E, \hat{\Omega})\psi(\vec{r}, E^*, \hat{\Omega}^*) + \\
+ \frac{1}{k_{\mathrm{eff}}} &\frac{\chi_{\mathrm{t}}(E)}{4\pi} \int_0^\infty \mathrm{d}E^* \nu_{\mathrm{t}}(E^*)\Sigma_{\mathrm{f}}(E^*)\phi(\vec{r}, E^*) \,.
\end{aligned}
\tag{1}
$$

Here, the notations are standard (Lewis and Miller Jr., 1993).

The solution of this problem gives the criticality eigenvalue k_{eff}, known as the effective multiplication factor, and the associated fundamental mode $\psi(\vec{r}, E, \hat{\Omega})$ (the angular neutron flux). The solution of this equation requires knowledge of the neutron interaction data, the (macroscopic) neutron cross sections, $\Sigma_x(E)$ and scattering kernels, $\Sigma_{\text{s}}(E, \hat{\Omega} \rightarrow E', \hat{\Omega}')$. For neutron energies E that are high compared with the chemical binding energies, the nuclei in the system can be considered free, *i.e.*, they can be described by using the classical Maxwell-Boltzmann distribution $n_{\text{MB}}(\vec{V}, T) \propto \exp(-M_i \vec{V}^2 / 2kT)$ with M_i being the mass of nuclide i. This approximation is called a free gas model (FG). Then only one set of cross sections is needed for each isotope i and each reaction x for a material at a given temperature T to build $\Sigma_x(E; T)$.

When neutrons are slowed down by collisions with the light nuclei used as moderators in thermal nuclear reactors and reach energies below the chemical binding energy of the molecules ($E \sim 1\text{-}10$ eV), the interaction with nuclides can no longer be considered as with a free Maxwellian gas. In this range of energy, the scattering cross sections vary according to the exchange of energy and momentum between the neutrons and the state of matter of reactor materials, such as, liquids and solids. Indeed, thermal neutrons with energy $E \simeq 25$ meV (corresponding to room temperature, $T \simeq 293.6$ K) have the de Broglie wavelength $\lambda \simeq 1.8$ Å, and these E and λ are very close to the characteristic energies of vibrational excitations and typical inter-atomic distances in the condensed phases of materials. Cold neutrons, with energies $E < 1\text{-}5$ meV (corresponding to $T \sim 10$ K) and wavelengths $\lambda > 4\text{-}9$ Å, match the characteristic length and time scales involved in self-diffusion processes in materials. Therefore, the scattering of low-energy neutrons in a material is sensitive to its atomic and molecular motion and structure, and results in specific inelastic/quasi-elastic effects for the energies and directions of the out-scattered neutrons. Thus, in principle, thermal neutron scattering cross sections and kernels are needed for each specific material used in applications, but, in nuclear engineering, they are of particular importance for moderators and reflectors, such as heavy/light water, graphite,

3

beryllium oxide, *etc.*

Accurate calculations of nuclear criticality are required both for the design of nuclear reactors and the verification of criticality safety conditions on systems that include significant amount of fissile materials. These calculations are based on usage of neutron interaction data, which are distributed in evaluated nuclear data libraries. For example, ENDF/B-VII.1 (Chadwick et al., 2011), the current released version of the ENDF evaluated nuclear data library, is an advance over previous versions of the library from the standpoint of the calculation of critical systems (Kahler et al., 2011). However, the criticality of a number of heavy water moderated critical systems still cannot be calculated within the experimental uncertainty of $\pm 1\sigma$ of the experimental value of k_{eff} (the effective multiplication factor). This is also true for modelling with other nuclear data libraries (Morillon et al., 2013; van der Marck, 2012).

The reasons for these discrepancies have been traced to imperfections of the modern evaluations for deuterium (Kozier et al., 2011; Morillon et al., 2013) and oxygen (Kozier et al., 2013; Roubtsov et al., 2014; Taylor and Hollenbach, 2013) but, for thermal systems, they could also be related to the thermal scattering cross sections of deuterium and oxygen bound in heavy water. In this paper, we use the CAB evaluation of the neutron thermal scattering kernel for liquid heavy water (Márquez Damián et al., 2014b), and present the results of nuclear criticality calculations for selected heavy water moderated and/or reflected benchmark systems that were added recently into the ICSBEP (Briggs, 2016) and IRPhEP (Bess, 2015) projects. The new benchmarks are based on recent measurements in the ZED-2 reactor (Chalk River, Canada) and sensitive to modifications of the scattering cross sections and kernels for deuterium and oxygen. Therefore, they are suitable for studying the impact of different evaluations of the thermal scattering kernel for heavy water on the value of k_{eff} of the thermal critical systems at zero power. Other (prior to 2012) international benchmarks with heavy water were analyzed in References (Morillon et al., 2013; Márquez Damián et al., 2014a). This study is a continuation and further

4

extension of Ref. (Márquez Damián et al., 2014a). For convenience and completeness of the presentation, portions of analysis from Refs. (Márquez Damián et al., 2014b,a) are included here.

2. Thermal scattering

For thermal neutrons, the scattering cross sections that appears in Eq. (1) are described in terms of a dimensionless function $S(\alpha, \beta)$ known as the *thermal scattering law* (TSL):

$$\Sigma_{\mathrm{s}}(E, \hat{\Omega} \to E', \hat{\Omega}') = \frac{\sigma_b N}{4\pi kT} \sqrt{\frac{E'}{E}} \, S(\alpha, \beta) \,. \tag{2}$$

Here α is a dimensionless positive parameter related to the neutron momentum transfer $\hbar \vec{q}$:

$$\alpha = \frac{E + E' - 2\sqrt{E'E}\mu}{AkT} = \frac{(\hbar \vec{q})^2}{2MkT} \,, \tag{3}$$

and β is a dimensionless parameter related to the energy transfer $\hbar\omega$:

$$\beta = \frac{E' - E}{kT} = -\frac{\hbar\omega}{kT} \,. \tag{4}$$

In these equations, $A = M/m_n$ is the nuclide-to-neutron mass ratio, μ is the neutron scattering cosine (in the laboratory frame), and other notations are standard (Williams, 1966; MacFarlane, 2010). The bound-state cross section σ_b is related to the free-atom cross section σ_f as $\sigma_b = \sigma_f(A+1)^2/A^2$, and, for all practical applications,

$$\sigma_f = \sigma_{\mathrm{s,th}}, \tag{5}$$

i.e., the free-atom cross section equals the tabulated thermal scattering cross section (at $E = 0.0253$ eV and $T = 0$ K) (Mughabghab, 2006). It is also assumed that the materials are isotropic (valid for molecular liquids) and the scattering kernel Σ_{s} satisfies the principle of detailed balance for neutron up-scattering ($\beta > 0$) and down-scattering ($\beta < 0$) probabilities, $S(\alpha, \beta) = \mathrm{e}^{\beta} S(\alpha, -\beta)$.

The scattering law is a property of the material, and depends on its dynamics and structure. (In condensed matter physics, the thermal scattering law $S(\alpha, \beta)$ is known

5

as the *dynamic structure factor*, $S(\vec{q}, \omega)$ (Lovesey, 1984), and $S(\alpha, \beta) \propto S(q, \omega)$, $\alpha \propto (\hbar \vec{q})^2$, $\beta \propto \hbar \omega$ (Farhi et al., 2015).) The scattering laws are calculated using models and approximations (such as perturbation theory) based on non-relativistic quantum mechanics and statistical physics. In the Gaussian incoherent approximation implemented in the nuclear data processing code NJOY, module LEAPR (MacFarlane, 1994), the dynamics of liquids is represented by a generalized frequency spectrum $\rho(\omega)$. For molecular liquids, the vibrational spectrum can be subdivided roughly into three major parts: intra-molecular (broadened molecular vibrations), inter-molecular (hindered rotations and translations, also called librations) and low-energy self-diffusion (translational) parts. The contribution of different atoms in the molecule can be distinguished by introducing partial $\rho_i(\omega)$ terms, similar to the partial phonon density of states in crystalline solids.

The structure of liquid can be introduced with the Sköld coherent correction (Sköld, 1967) for nuclide i that is present in a given liquid and can scatter neutrons coherently (*i.e.*, $\sigma_{\mathrm{coh},i} \neq 0$, $\sigma_{\mathrm{coh},i} + \sigma_{\mathrm{incoh},i} = \sigma_{\mathrm{s},i}$). For isotropic molecular liquids, the knowledge of partial (static) structure factors (Soper, 2013) $S_{ij}(q)$ (or radial correlation functions $g_{ij}(r)$) is required to obtain the Sköld correction factors $\tilde{S}_i(q)$ (*e.g.*, i, j = H, O for H_2O or D, O for D_2O). For the neutron scattering by ^{1}H in hydrogenous materials, one can disregard the coherent corrections and use the incoherent approximation for the scattering kernel $S_{\mathrm{H}}(\alpha, \beta)$. For the thermal neutron scattering by ^{2}H($\equiv$ D) in deuterated liquids, the incoherent approximation is, strictly speaking, not applicable, $\sigma_{\mathrm{coh}}(^2\mathrm{H}) \gtrsim \sigma_{\mathrm{incoh}}(^2\mathrm{H})$, $\sigma_{\mathrm{coh}}(^2\mathrm{H})/\sigma_{\mathrm{s}}(^2\mathrm{H}) \approx 0.73$ (Mughabghab, 2006). In the nuclear data processing code NJOY, the Sköld method is implemented, and one can calculate the coherent inelastic part of the scattering kernel $S_{\mathrm{D}}(\alpha, \beta)$ provided the partial structure factors of the molecular liquid are available as external data structures (*e.g.*, q, $S_{\mathrm{DD}}(q)$, $S_{\mathrm{OD}}(q)$, and $S_{\mathrm{OO}}(q)$); see (Soper, 2013) and references therein).

The modern thermal scattering laws are distributed in the evaluated nuclear data libraries, as part of the thermal scattering sublibrary (see, for example, Refs. (Chad-

wick et al., 2011; MacFarlane and Kahler, 2010)), following the ENDF-6 format (Trkov et al., 2011) for representing the numerical data. Nuclear data processing codes, such as NJOY (MacFarlane and Muir, 1999) and GRUCON (Sinitsa and Rineiskij, 1993), are expected to read and post-process the thermal scattering sublibrary data files.

3. Thermal scattering libraries for heavy water

3.1. Existing libraries (1970 – 2010)

The evaluated nuclear data libraries include scattering law files for heavy water produced from two essentially different models: one initially published by Koppel and Young at *General Atomics* (Koppel and Houston, 1978) (GA model), and another proposed by Keinert and Mattes at *Institut für Kernenergetik und Energiesysteme*, Stuttgart (Keinert et al., 1984; Mattes and Keinert, 2005) (IKE model).

The IKE model includes several improvements over the GA model. While both models are based on frequency spectra originally measured by Haywood in the 1960s (Haywood, 1967), the IKE model incorporates newer measurements which include temperature dependence, $\rho(\omega; T)$. The IKE model also includes a correction for the coherent component of the scattering in deuterium, whereas the incoherent approximation is used in the GA model. However, the IKE coherent correction is not complete, because it only includes the D$-$D partial structure factor $S_{\mathrm{DD}}(q; T)$ obtained from modelling (numerical simulations) and using simplified (Lennard-Jones type) interaction potential for atoms. In both models, the translational self-diffusion of the liquid is approximated as a molecular free-gas motion. This is equivalent to assuming the zero-width asymptotic behaviour of $\rho(\omega)$ of the liquid at small ω:

$$\rho(\omega) \sim w_t(T)\, \delta(\omega) + \rho_{\mathrm{reg}}(\omega) \ \text{ at } \ \omega \to 0 \ \ (\hbar\omega \ll kT). \tag{6}$$

Here, w_t is the translational weight of the generalized vibrational spectrum and ρ_{reg} is the regular part of $\rho(\omega)$ that satisfies $\rho_{\mathrm{reg}} \to 0$ as $\omega \to 0$. In the IKE model, $w_t(T) = 0.05$ for deuterium in the liquid heavy water. However, in more realistic dynamic models with

7

the translational self-diffusion, there is no sharp feature in $\rho_i(\omega)$ at $\hbar\omega \ll kT$, and $\rho_i(\omega) \sim$ const > 0 as $\omega \to 0$ (Marti et al., 1996; Lisichkin et al., 2005).

Oxygen is treated as a free atomic gas at a given temperature T in both models. For the light water (H_2O), this is a well-justified approximation because the scattering cross section of oxygen is small compared to the cross section of ^1H and the (incoherent) neutron scattering in hydrogen is predominant. For heavy water, $\sigma_s(^2H) \simeq \sigma_s(^{16}O)$ (Mughabghab, 2006), and both D and O components have similar importance. Moreover, even-even nuclei (^{16}O and ^{18}O) constitute 99.96% of natural oxygen, causing coherent neutron scattering (which is not included in the free gas approximation) to be predominant, and the coherent scatterer ^{16}O is the main oxygen scatterer in D_2O[1]. Thus, there are several key improvements that could be made in the thermal scattering laws for heavy water given in the modern evaluated nuclear data libraries.

There is always a small admixture of ^1H in reactor-grade (high purity) heavy water (with purity > 99.0 wt.% D_2O, $n(^1H)/n(^2H) \simeq 10^{-3}$-$10^{-2}$). In chemical equilibrium and with no external radiation, almost all hydrogen in the heavy water is in the form of HDO molecules (Bayly et al., 1963; Kim et al., 2011) (and so each HDO in liquid heavy water is bounded by hydrogen bonds into a cluster of D_2O molecules). In the evaluated nuclear data libraries, there is no special thermal scattering law for ^1H in HDO in heavy water. In practical applications, such as modeling neutron transport in critical systems, the effects of chemical bonding of ^1H in the heavy water of known purity is usually taken into account by applying the thermal scattering laws for ^1H in the light water (H_2O). It seems that this approximation does not introduce a significant bias or noticeable discrepancy to the estimates of k_{eff} for the critical systems with reactor-grade heavy water. Nevertheless, the development of a new thermal scattering law for ^1H in HDO is warranted for better modelling of heavy water of low purity and heavy water / light water mixtures.

---

[1]In fact, in heavy water of high (reactor-grade) purity, the relative concentrations of ^{17}O and ^{18}O can be different from their natural abundance values; see Ref. (Gray and Guest, 1986) for detail.

8

For completeness, we mention the efforts by Edura, Morishima of Kyoto University and their collaborators (Morishima and Aoki, 1995; Edura and Morishima, 2005, 2006) to improve the light/heavy water models and generate new neutron scattering kernels, mainly for neutron cold source applications. The Kyoto University results are distributed in *CLES*, or Cross Section Library of Moderator Materials for Low-Energy Neutron Sources (Edura and Morishima, 2006; Morishima, 2006). However, the scattering kernels and cross sections for light/heavy water are not given in the ENDF-6 format, and they are not separated into the main nuclide contributions, *e.g.*, for ^{2}H ($S_D(\alpha, \beta; T)$), ^{16}O ($S_O(\alpha, \beta; T)$), and ^{1}H ($S_H(\alpha, \beta; T)$), to describe thermal neutron scattering on (reactor-grade) heavy water (D_2O & HDO). Therefore, it is not straightforward to implement CLES evaluations of the neutron scattering laws of light/heavy water into modern neutron transport codes and their (application-specific) nuclear data libraries because such cross section libraries are generated using NJOY (MacFarlane and Kahler, 2010) (or similar nuclear data processing codes) directly from the nuclear data sub-libraries distributed in the ENDF-6 format.

3.2. CAB evaluation

The TSL libraries for water based on the *CAB models* are described in detail in Ref. (Márquez Damián et al., 2014b), and additional details for heavy water are given in Refs. (Márquez Damián et al., 2014a, 2015) to which we refer the interested readers.

The CAB evaluations are based on the results of molecular dynamics simulations (MD) combined with the usage of recent experimental data and the capabilities of LEAPR module of NJOY 2012 (MacFarlane and Kahler, 2010) to generate the TSL's in the ENDF-6 format. To improve over the existing libraries for heavy water available in the evaluated nuclear data libraries (ENDF/B-VII.1, JEFF-3.2, JENDL 4.0), MD simulations (Márquez Damián et al., 2013) using GROMACS (Van Der Spoel et al., 2005) were performed to calculate the frequency spectrum $\rho_i(\omega; T)$ for deuterium and oxygen in liquid heavy water at different temperature and pressures relevant for practical applications. It is known (Marti et al., 1996; Lisichkin et al., 2005) that the modern MD simulation packages are capable

9

of predicting accurately the vibrational frequency spectra of light and heavy water using flexible models of water (González and Abascal, 2011), provided the simulations run long enough to cover the translational self-diffusion time scale $\simeq 10$ ps that is expected to be of the same order of value as the translational correlation time, $\tau_t \simeq 7$ ps (Bée, 1988), and the MD time step dt is chosen small enough to resolve the intra-molecular vibrations ($dt \simeq 0.1$ fs). Then, the frequency spectra $\rho_{\mathrm{D}}(\omega)$ and $\rho_{\mathrm{O}}(\omega)$ can be calculated using a Fourier transform of the velocity autocorrelation functions for deuterium and oxygen obtained from the MD description of $N \gg 1$ molecules of water at each time step t_n, *i.e.*, from $(\mathbf{v}_i(t_n), \mathbf{r}_i(t_n))$ trajectory data. The results reported in this study are based on using an implementation of the TIP4P/2005-flexible water model (González and Abascal, 2011) for $N = 512$ of D_2O molecules in GROMACS 4.6, with $dt = 0.1$ fs and the MD simulation time of ≈ 100 ps.

Similarly to $\rho_i(\omega; T)$, partial structure factors $S_{ij}(q; T)$ were calculated from GROMACS simulations using a Fourier transform of the pair correlation functions $g_{ij}(r; T)$ (Soper, 2013) that were also estimated from the MD description (trajectories) of N molecules of (heavy) water at given thermodynamic conditions (N, V, T, p). The obtained structure factors were validated using the results of measurements by Soper *et al.* (Soper and Benmore, 2008). Then the Sköld correction factors for deuterium and oxygen scattering kernels, $\tilde{S}_{\mathrm{D}}(q; T)$ and $\tilde{S}_{\mathrm{O}}(q; T)$, were built up using the polyatomic Vineyard's approximation (Vineyard, 1958). In this study, we do not discuss the case of pressurized heavy water used in power nuclear reactors and we use the CAB evaluations at room temperature ($T = 293.6$ K) and normal pressure (1 atm).

The CAB $S(\alpha, \beta)$ libraries were validated by comparison with many single-neutron scattering observables obtained experimentally over years of studying the interaction neutrons with water, and some improvements were found over the thermal scattering law files available in the modern evaluated nuclear data libraries (Márquez Damián et al., 2014b).

To analyze the effects of the CAB TSL libraries on critical systems, we compare the

selected experimental results of the total neutron cross section for heavy water (Kropff et al., 1974), including the recently measured ones (Márquez Damián et al., 2015), with the calculations using our model (CAB), the ENDF/B-VI (GA model), and the ENDF/B-VII.0 (= ENDF/B-VII.1, based on IKE model); see Fig. 1 . For the evaluated TSL data, the incident energy E varies from the ultra-cold ($E \simeq 1~\mu$eV) to epi-thermal ($E \simeq 10\text{-}20$ eV) neutron energies. Although the improvement found at cold neutron energies ($E \simeq 1$ meV) is important, the neutron flux expected in the thermal critical systems is low at these energies. For example, in heavy water, we expect that the neutron flux is $\phi(E) \propto E \exp(-E/kT_{\text{eff}})$ at $E < 0.1\text{-}1.0$ eV with the neutron effective temperature $kT_{\text{eff}} \approx kT \approx 25$ meV at the room temperature. Thus the improvement for cold neutrons would have little impact on the thermal critical systems. To validate the model predictions at ultra-cold neutron energies ($E \simeq 1\text{-}10~\mu$eV), new measurements with high-purity heavy water would be desirable. (Indeed, some (uncontrollable) amount of light water (H_2O) mixed with D_2O can drive the results of σ_{tot} up.) On the other hand, the improvements at thermal neutron energies ($E \simeq 10\text{-}30$ meV; see Fig. 1) have more importance from the thermal critical systems because the neutron flux is higher in this energy range. Similar results for heavy water were demonstrated in Refs. (Farhi et al., 2015) and (Edura and Morishima, 2006).

In the ENDF-6 format, the thermal scattering libraries ($S(\alpha, \beta)$ data) are given in a tabulated form on the finite grid of α_n and non-negative β_m. As the standard evaluations of thermal scattering kernels for liquids should work in a wide incident energy range, from $E = 10^{-5}$ eV to $E \simeq 5\text{-}10$ eV, the choice and size of such grids have to be carefully examined for each particular material to describe as accurately as possible the phase space of out-scattered neutrons typically expressed in terms on the allowed momentum and energy transfer, q and $\hbar\omega$. In the CAB model of liquid D_2O, $\dim(\alpha_n) = 501$ and $\dim(\beta_m) = 501$. For example, to describe the quasi-elastic peak in the energy distributions of out-scattered neutrons at small momentum transfer (e.g., $q \sim 0.1~\text{Å}^{-1}$), it is necessary to refine the grid at $\alpha \simeq \beta \to 0$ to resolve the energy transfers of less than $\simeq \hbar\mathcal{D}q^2 \simeq 10^{-6}$ eV. (Here, $\mathcal{D}$ is

11
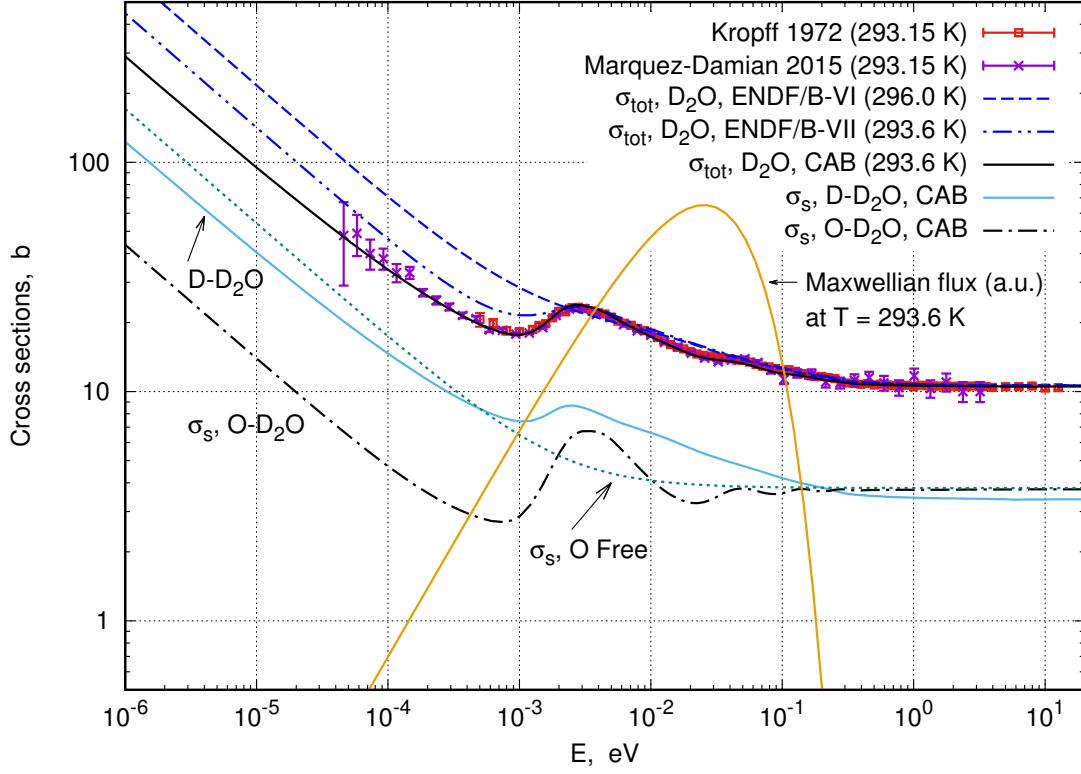
Figure 1: Total cross sections for heavy water (per molecule) at room temperature *vs.* incident neutron energy E ($10^{-6}\,\mathrm{eV} < E < 20.0\,\mathrm{eV}$). Experimental results (Kropff et al., 1974; Márquez Damián et al., 2015) are compared with calculations using the CAB model, ENDF/B-VII (IKE model), and ENDF/B-VI (GA model). The Maxwellian neutron flux for $T_\mathrm{eff} = 293.6$ K (0.0253 eV), which would be expected for fully thermalized neutrons, is shown for reference. The differences in the evaluated σ_tot can be traced to the scattering cross sections of O in D_2O; compare the curves at the bottom that show the scattering cross sections of ^{2}H and ^{16}O.

the diffusion coefficient of heavy water, $\mathcal{D} \simeq 0.2\ \text{Å}^2/\text{ps}$.) This requires $\beta_m \sim 10^{-5}\text{-}10^{-6}$. Following Ref. (Mattes and Keinert, 2005), the maximum value of β_m can be chosen as

$$\beta_\mathrm{max} \simeq E_b/kT, \ \ E_b \approx 4.8 \text{ eV}. \tag{7}$$

Here E_b is the (covalent) bond energy of D_2O molecule, and so $\beta_\mathrm{max} \approx 158$ at the room temperature. However, to improve the description of cases with large energy transfer (deep inelastic scattering), the grid is extended beyond β_max up to $\beta^\star \approx 395$ in the CAB model.

Then the maximum of α_n is chosen as $\alpha^\star \approx \beta^\star/A$.

For large energy (momentum) transfer outside of the tabulated $S(\alpha_n, \beta_m)$ data (*e.g.*, for $|\beta| > \beta^\star$ and/or $\alpha > \alpha^\star$), it is recommended (Trkov et al., 2011) using the short-collision-time approximation to estimate the value of $S(\alpha, \beta)$ (Mattes and Keinert, 2005; MacFarlane, 1994). To apply this approximation, one has to estimate the effective temperature of a neutron scatterer $T_{\text{eff}, i}$,

$$kT_{\text{eff}, i} = \int_0^\infty (\hbar\omega/2) \coth(\hbar\omega/2kT) \, \rho_i(\omega) \, d\omega \,. \tag{8}$$

Here we assume that $\rho_i(\omega)$ is normalized to unity. The differences among the above-mentioned models of thermal neutron scattering in water are noticeable if we compare the effective temperatures of hydrogen (D for heavy water) and oxygen and also the relative contributions of different components of $\rho_i(\omega)$ into the value of $T_{\text{eff}, i}$. For example, in the CAB model, we have $T_{\text{eff}, D} \approx 865$ K (74.5 meV) and $T_{\text{eff}, O} \approx 454$ K (39.1 meV) at the room temperature $T = 294$ K (25.3 meV). For deuterium, our result is lower than the IKE (ENDF/B-VII) effective temperature, $T_{\text{eff}, D} \approx 1010$ K (87.0 meV) at the room temperature, mostly as a result of re-evaluation intra-molecular part of $\rho_D(\omega)$ ($E > 120$ meV). In the free gas approximation for neutron scattering by oxygen, it is always $T_{\text{eff}, O} = T$. However, oxygen bound in the liquid D_2O at the temperature T is noticeably "hotter", from the stand point of out-scattered neutrons. The effective temperatures for deuterium and oxygen in heavy water can be measured using deep inelastic scattering technique (Dawidowski et al., 2016), and agreement between the predictions of CAB model and recent measurements of $T_{\text{eff}, i}$ was found to be very good; see Ref. (Dawidowski et al., 2016) for detail.

The CAB TSL libraries have been presented to the Cross Section Evaluation Working Group (CSEWG, USA) (Roubtsov, 2015) and are currently available for testing in the ENDF/A GForge server (USNDP/CSEWG GForge Collaboration Server, 2017) to be included into the forthcoming release of the ENDF/B evaluated nuclear data library.

3.2.1. Average scattering cosine and energy

Beside the scattering cross sections, thermal scattering kernels (2) can be characterized by other integral parameters obtained by averaging the scattering cosine and energy of out-scattered neutrons, μ and E'. The values of $\langle\mu\rangle$ (also called mu-bar) and $\langle E'\rangle$ (also called E-bar) give a general idea of how a given material scatters cold, thermal, and epi-thermal neutrons. They are used to estimate the transport-corrected macroscopic cross sections and other relevant parameters in the analysis of slowing down and thermalization of neutrons (Lewis and Miller Jr., 1993; MacFarlane, 2010). In this study, we calculate also the higher moments, such as $\langle\mu^2\rangle$ and $\langle E'^2\rangle$, to have a rough idea about deviations from the averages in angular and energy distributions,

$$d\langle\mu\rangle = \sqrt{\langle\mu^2\rangle - \langle\mu\rangle^2}, \;\; d\langle E'\rangle = \sqrt{\langle E'^2\rangle - \langle E'\rangle^2}\,. \tag{9}$$

The average scattering cosine (normalized per molecule, D_2O) is shown in Fig. 2 as a function of E for the CAB and free gas models. It is a weighted sum of the individual components, $\langle\mu\rangle(D\text{-}D_2O)$ and $\langle\mu\rangle(O\text{-}D_2O)$, with the weights equal to $2 \times \sigma_s(D\text{-}D_2O)$ and $\sigma_s(O\text{-}D_2O)$, respectively. The experimental data (Beyster et al., 1965; Kornbichler, 1965) are also shown in Fig. 2 and agreement is good. Roughly, the relative fraction of $\approx 50\text{-}60\%$ of all out-scattered neutrons goes into the interval $(\langle\mu\rangle - d\langle\mu\rangle,\ \langle\mu\rangle + d\langle\mu\rangle)$ that is shown in Fig. 2 by dashed lines. We notice that at $E > 1$ eV, the average values of $\langle\mu\rangle$ and $\langle\mu^2\rangle$ are almost the same in the both models. For example, the epi-thermal asymptotic value for $\langle\mu\rangle$ in the free gas model is $\langle\mu\rangle(2D + O)) \approx 0.23$ (estimated at $T = 0$ K) and it is evident in Fig. 2 as the both models approach this asymptotic value at $E \gtrsim 1$ eV. On the other hand, for $E \to 0$ ($E \ll kT$), we have $\langle\mu\rangle \to 0$, *i.e.*, the ultra-cold neutrons are scattered isotropically. The difference between the free gas and liquid scattering is evident for the thermal and cold neutrons. We suggest that new experimental data for $\langle\mu\rangle$ (and/or detailed angular distributions) at $E \simeq 2$ meV would be desirable to reveal the features of back-scattering ($\mu < 0$, with $\mathrm{acos}(\langle\mu\rangle) \simeq 104°$) of the cold neutrons on liquid D_2O at ambient temperatures and pressures. (Recently, the neutron angular distributions

were measured at $E = 44$ meV using the neutron beam from the NRU Reactor at Chalk River (Li et al., 2017).)

The average energy E' (normalized per molecule, D_2O) is shown in Fig. 3 as a function of E for the CAB and free gas models. Similarly to $\langle \mu \rangle$, $\langle E' \rangle (D_2O)$ is a weighted sum of the individual components, $\langle E' \rangle (D\text{-}D_2O)$ and $\langle E' \rangle (O\text{-}D_2O)$. We notice that the slowing-down regime ($\langle E' \rangle < E$) is valid for the epi-thermal neutrons with $E > 1\text{-}4$ eV. (The epi-thermal asymptotic values for $\langle E' \rangle (A)$ scale linearly with E as $\text{const}(A) \times E$ at $T = 0$ K.) At room temperature, the neutron up-scattering constitutes $\lesssim 1\%$ of all out-scattering events $E \to E'$ at $E \gtrsim 1$ eV. As neutrons are getting more thermal, the neutron up-scattering weight is increased. The relative up-scattering faction of $\gtrsim 10\%$ occurs at $E < 0.5$ eV, and the up-scattering dominates ($> 50\%$) at $E \lesssim 0.05$ eV. In addition, the cross-over area ($\langle E' \rangle \approx E$) is found near $E \simeq 0.05$ eV at the room temperature. As $E \to 0$ ($E \ll kT$, $i.e.$, ultra-cold neutrons), $\langle E' \rangle (D_2O)$ approaches the value of $\simeq kT$.

The difference between the free gas and liquid scattering is evident if we examine how $\langle E' \rangle$ and $\langle E' \rangle \pm d\langle E' \rangle$ change with the energy decrease at $E < 0.1$ eV; see Fig. 3. In particular, the differences at $E \simeq 1\text{-}10$ meV are evident. Using the estimates of $\langle E'^2 \rangle$ $vs.$ E, we calculate the relative neutron scattering fraction of scattering into the energy interval ($\langle E' \rangle - d\langle E' \rangle$, $\langle E' \rangle + d\langle E' \rangle$) shown in Fig. 3 by dashed lines. In the slowing-down regime ($E > 1$ eV), it is $\simeq 55\text{-}60\%$ and, with the decrease of incident energy, this fraction is increased up to $\simeq 80\text{-}90\%$ for the thermal and cold neutrons.

4. Criticality benchmarks (ZED-2 reactor)

The *International Criticality Safety Benchmark Evaluation Project* (ICSBEP) (Briggs, 2016) is a NEA-OECD project dedicated to compile, analyze and formally document critical experiments to be used as benchmarks for nuclear data, criticality safety, shielding, and reactor calculation codes. At the moment of writing, the product of this effort is 567 reports or *evaluations* containing information on 4913 critical configurations, compiled in the *International Handbook of Evaluated Criticality Safety Benchmark Experiments*,
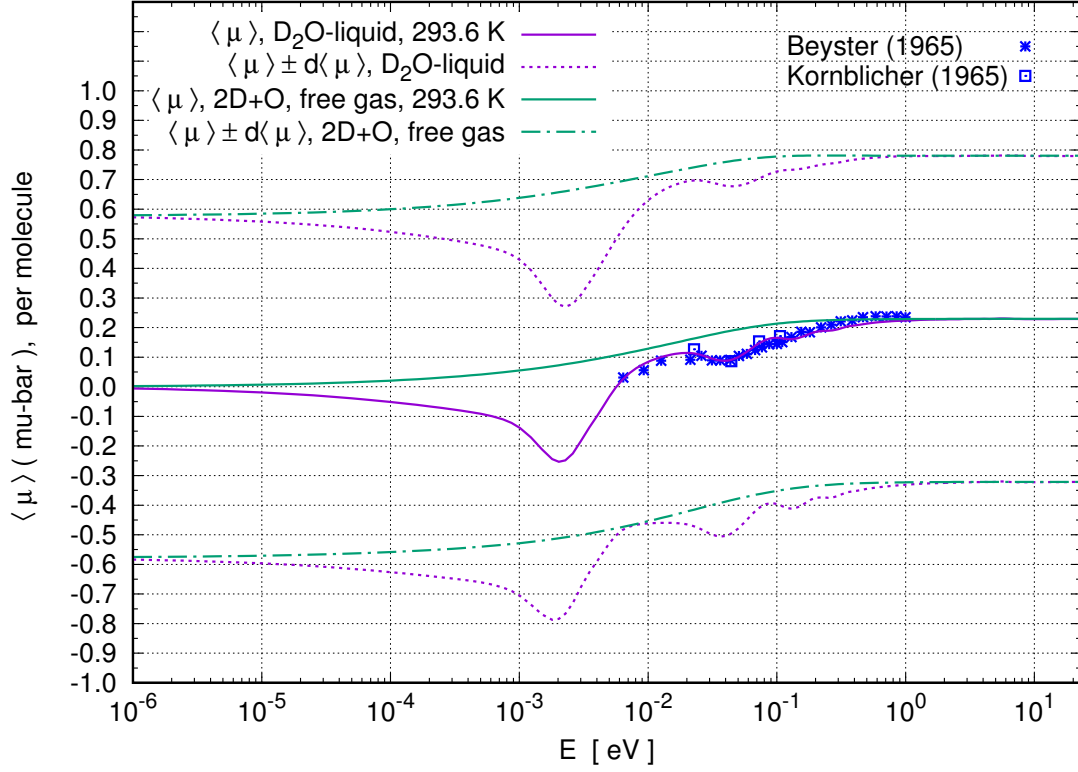
Figure 2: Average scattering cosine $\langle\mu\rangle(D_2O)$ is calculated against the incident neutron energy E using the CAB model at the room temperature and compared with experimental data (Beyster et al., 1965; Kornbichler, 1965). The results obtained using the free gas model for $2D + O$ are shown for comparison. The deviations from the average values are also shown for the both models by plotting $\langle\mu\rangle \pm d\langle\mu\rangle$ (dashed lines).

distributed as a DVD. Similarly, the *International Reactor Physics Experiment Evaluation Project* (IRPhEP) (Bess, 2015) is an NEA-OECD project with an emphasis on reactor core experiments (including some power reactor configurations). It includes 143 experimental series performed at 50 nuclear facilities (as of the 2015 Edition of the IRPhEP Handbook).

These evaluations (benchmarks) include a description of all the important physical parameters (dimensions, compositions, temperature), and analyses of the effect of their uncertainties in the multiplication factor of the system. For each system, a multiplication factor is given with its corresponding uncertainty, $k_{\text{eff}}^{\text{bench}} \pm \delta k_{\text{bench}}$. Despite the system
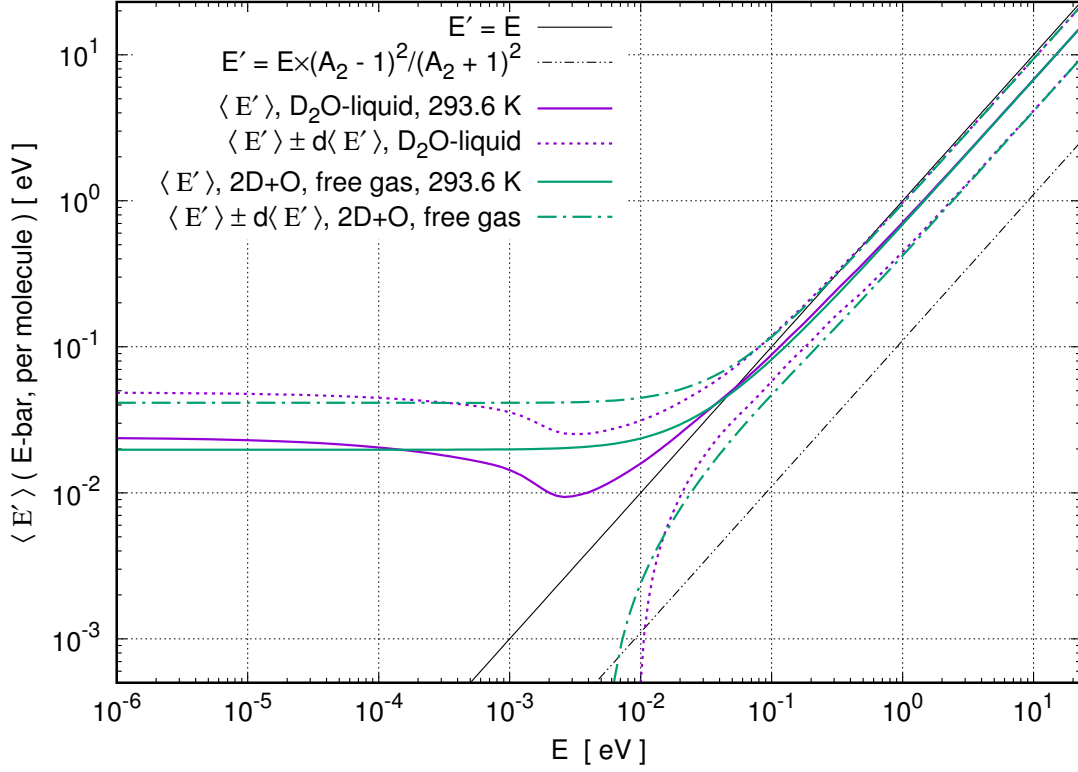
Figure 3: Average energy of out-scattered neutrons $\langle E'\rangle(D_2O)$ is calculated against the incident neutron energy E using the CAB model at the room temperature. The results obtained using the free gas model for $2D + O$ for comparison. The deviations from the average values are also shown for the both models by plotting $\langle E'\rangle \pm d\langle E'\rangle$ (dashed lines). A_2 is the short notation for $A(^2H)$, and the line $E' = E(A_2 - 1)^2/(A_2 + 1)^2$ represents the lower cut-off of kinematically allowed E' for the out-scattered neutrons in the $^2H(n,n)$ reaction at $T = 0$ K.

being critical ($k_{\text{eff}}^{\text{exp}} = 1.0$), the multiplication factor of a model ($k_{\text{eff}}^{\text{bench}}$) might not be unity if simplifications were introduced in the preparation of the benchmark. The uncertainty associated to the multiplication factor includes not only the experimental error, but also the effect of the uncertainties in the parameters of the system (so that $\delta k_{\text{bench}} \geq \delta k_{\text{exp}}$).

To study the effect of the new CAB libraries on criticality calculations, we selected a series of heavy water moderated experiments from the ICSBEP Handbook and documented the results in Ref. (Márquez Damián et al., 2014a). However, both the ICSBEP and IR-

PhEP projects are constantly expanding and new benchmarks are becoming available for all interested researchers. In particular, a new relevant benchmark was added into the ICS-BEP Handbook: LEU-MET-THERM-003, a simple critical assembly moderated by heavy water (Atfield, 2016). This benchmark can be compared with similar configurations, such as, for example, LEU-MET-THERM-001; see Table 1. Another heavy water benchmark was added into the IRPhEP collection: ZED2-HWR-EXP-001 (Atfield, 2015). The new heavy water benchmarks are based on recent crtitical experiments with the ZED-2 reactor located at Chalk River, Canada.

ZED-2 is a reactor of the calandria vessel type. As shown in Figure 4, it is a cylindrical tank made from Al with a sidewall thickness of 0.64 cm and a bottom thickness of 2.7 cm. The calandria has a 3.36-m diameter and 3.30-m depth. It is surrounded by graphite blocks arranged with an average thickness of 60 cm radially and 90 cm below the tank. Fuel assemblies are hung vertically from beams located above the calandria. The reactor is made critical by pumping heavy water moderator into the calandria, and the reactor power is controlled by adjusting the moderator level. Typical moderator critical levels range between 120 and 250 cm above the reactor tank floor. The maximum power is 200 watts (nominal), corresponding to an average neutron flux of about $10^9 \mathrm{\,n\,cm}^{-2}\mathrm{s}^{-1}$. Typical experimental data are moderator critical heights and core conditions that include the temperature and purity of the (reactor-grade) heavy water being used to achieve criticality. Then an analysis of these data is performed using a reference-level neutron transport code, such as the Monte Carlo N-Particle (MCNP) code (X-5 Monte Carlo Team and Brown, 2005), with a nuclear data library derived from one of the latest evaluated nuclear data libraries, *e.g.*, the ENDF/B-VII evaluation (Chadwick et al., 2006, 2011).

4.1. Basic settings for MCNP modelling

As a baseline, all models of the critical systems were calculated using the KCODE mode of MCNP5 v. 1.60 (X-5 Monte Carlo Team and Brown, 2005) and the continuous-energy cross section data library based on the ENDF/B-VII.0 evaluation (Chadwick et al., 2006;

18
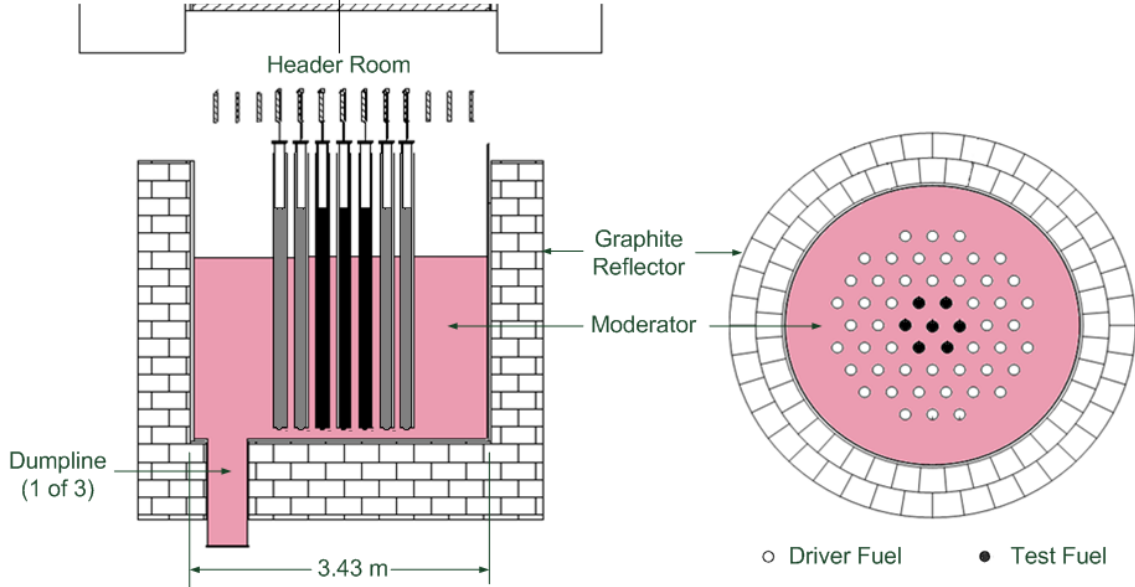
Figure 4: Schematic view of ZED-2 reactor moderated by heavy water.

Altiparmakov, 2010). For the selected heavy water benchmarks with natural uranium based fuel, (Table 1) the latest version of MCNP, MCNP6 v. 1 (Goorley et al., 2012), and its nuclear data library based on the ENDF/B-VII.1 evaluation (Chadwick et al., 2011) show the same trend and give basically the same results as the baseline MCNP options chosen in this study (van der Marck, 2006, 2012).

The KCODE algorithm in MCNP performs reactor criticality calculations and requires neutron cross section data for the neutron propagation simulation in the energy range 10^{-5} eV $\leq E \leq$ 20 MeV. As an option, one can include additional thermal scattering files ($S(\alpha, \beta)$ data) to take into account the chemical and liquid/solid-state bonding effect of the nuclides of interest in particular materials. Then the free-gas scattering kernels of these nuclides are replaced by the $S(\alpha, \beta)$ data below a certain cut-off energy, *i.e.*, for the incident neutron energies E from

$$10^{-5} \text{ eV} \leq E \leq E^*, \ \ E^* \simeq 5\text{-}10 \text{ eV}. \tag{10}$$

Here, E^* is the upper energy cut-off for the $S(\alpha, \beta)$ treatment of neutron scattering in the MCNP simulations. For the CAB libraries, we use $E^* = 10.0$ eV for ^{2}H and ^{16}O in heavy water, and for ^{1}H in light water. The conversion from the thermal scattering laws in the ENDF-6 format to the $S(\alpha, \beta)$ data files that MCNP can read and process was done using NJOY 2012 (MacFarlane and Muir, 1999; MacFarlane and Kahler, 2010) with in-house patches developed to improve the numerical accuracy while processing large $S(\alpha, \beta)$ data files. To insure the consistency with the ENDF/B-VII.0 and VII.1 evaluations, the CAB scattering laws of D-D$_2$O and O-D$_2$O (MF7, MT4) were normalized to $2 \times \sigma_{\text{free}}(^2\text{H}) = 6.790$ b and $\sigma_{\text{free}}(^{16}\text{O}) = 3.852$ b, respectively. (The subdivision of scatterers into principal and non-principal ones is not used in the CAB model of D$_2$O.)

In Monte Carlo simulations of neutron scattering events in the thermal energy region, an algorithm has to choose the energy and direction of out-scattered neutrons by reading an external data file (called thermal ACE file) and then apply a proper estimator. This happens, for example, if a neutron with energy E interacts with a nuclide i in the material $=$ *heavy water* (at a given temperature T), and the reaction channel is chosen to be the neutron scattering on $i = {}^2$H, and $E < E^*$, and the file $S_\text{D}(\alpha, \beta; T)$ exists in the nuclear data library in the form of thermal ACE file. As sampling of the out-scattering characteristics has to be made computationally fast, the algorithm often assumes that the double-differential cross sections are pre-processed in a certain way: the angular (μ) and energy (E') distributions are usually cast into the probability tables based on equal binning of the probability distribution functions $P_s(E \to E', \mu; T)$. We use 64 equi-probable angular bins (in μ) and 500 equi-probable energy bins to represent the distributions in μ and E' in the $S^{(\text{CAB})}(\alpha, \beta)$ libraries for the light and heavy water to be applied with MCNP[2]. It is anticipated that such thermal ACE files can be used in modelling both the experimental

---

[2]In NJOY, the default option for the secondary energy bins was used. Then, the code generates variable weights that are skewed toward the first two and last two bins in a row as follows: $w_i(E') \propto 1, 4, 10, 10, \ldots, 10, 4, 1$.

Table 1: Selection of ICSBEP / IRPhEP criticality benchmarks used in this study.

Evaluation ID	# of Cases	Title
LEU-MET-THERM-001	1	RB Reactor: Natural Uranium (NU) Rods in Heavy Water
LEU-MET-THERM-003	3	ZED-2 Reactor: a lattice of NU ZEEP Rods in Heavy Water
ZED2-HWR-EXP-001	8	D_2O Moderated Lattice of NU UO_2 28-Element Fuel Assemblies in ZED-2 reactor

neutron scattering set-ups, in which the multiple-scattering events in the targets (cells with water) are not desirable, and the heterogeneous reactor cores, in which neutrons experience a large number ($\simeq 100$) of collisions in moderators/reflectors.

MCNP6 (Goorley et al., 2012) accepts the $S(\alpha, \beta)$ tables with continuous representation of the probability distribution functions in the energy E'. Although the impact of the MCNP6-compatible $S(\alpha, \beta)$ tables (continuous thermal ACE files) on the estimates of principal eigenvalues (k_{eff}) for the critical systems is found to be small in modelling the assemblies with heavy water ($|k_{\text{eff}}(\text{MCNP6}\, S(\alpha, \beta)) - k_{\text{eff}}(\text{MCNP5}\, S(\alpha, \beta))| \lesssim 10$ pcm), the asymptotic behaviour of the corresponding eigenvectors, $\phi(E, \mathbf{r})$ at low energies ($E < kT$), is better with the continuous representation of $S(\alpha, \beta)$ tables (MacFarlane and Kahler, 2010). For example, the calculated energy-resolved neutron spectra in heavy water are free of irregularities and numerical artifacts at $E < 0.01$ eV and scale as $\propto E^2 \exp(-E/kT_{\text{eff}})$.

The MCNP models of the ZED-2 benchmarks with heavy water were run until a statistical uncertainty $\delta k^{\text{calc}} \approx \pm 4\text{-}5$ pcm was achieved (1σ), which is small compared with the benchmark uncertainties, $\delta k_{\text{MCNP}}^{\text{calc}} \ll \delta k_{\text{bench}}$. (Recall that 1 pcm and 1 mk are the changes in k_{eff} by 1.0×10^{-5} and 1.0×10^{-3}, respectively; 1 mk = 100 pcm.)

4.2. Results

As the calculations using the ENDF/B-VII library tend to overestimate the multiplication factor of heavy water moderated systems (van der Marck, 2006), we anticipate that changing the ENDF/B-VII $S(\alpha, \beta)$ library for ^{2}H in liquid D_2O to the CAB model for ^{2}H and ^{16}O will reduce the criticality of the heavy water benchmarks in the most cases.

4.2.1. LEU-MET-THERM-003

The ZED-2 critical cores described in the LEU-MET-THERM-003 benchmark (Atfield, 2016) consist of three hexagonal lattices of uranium metal rods in aluminum cladding (called ZEEP rod for historical reasons) moderated by heavy water. The lattice pitch varies from 20.0 to $\approx$ 23.0 cm. The results of the criticality calculations of LEU-MET-THERM-003 (ZEEP Rod benchmark) are shown in Fig. 5: the expected experimental value (the benchmark multiplication factor k_{eff}) and the calculated one given as a function of the lattice pitch. These results were computed using ENDF/B-VII.0 based libraries for all isotopes, with the exception of the thermal scattering libraries for deuterium and oxygen, which were replaced with the new $S(\alpha, \beta)$ model. The results obtained using the free gas approximation for heavy water are also shown in Fig. 5 to emphasize that this benchmark is sensitive enough to the differences resulting from the $S(\alpha, \beta)$ thermal scattering treatment for the neutrons interacting with deuterium and oxygen bounded in the heavy water. Indeed, the free gas model for heavy water (moderator and reflector) introduces a negative bias in k_{eff} of $\approx$ 1000 pcm $> \delta k_{\text{bench}}$ ($k_{\text{bench}} = 1.0$). The differences between free gas and $S(\alpha, \beta)$ models can be seen in the neutron spectra as well. In Fig. 6, we show the neutron spectra ($\propto E \times \phi(E)$) in the fuel rods (U metal), moderator and reflector (heavy water). We note that the position of maxima (at $E^\star = 2T_{\text{eff}}$) and the widths of the thermal part of neutron spectra are not changed significantly upon FG $\rightarrow S(\alpha, \beta)$ for D_2O, although the thermal peaks are getting stronger upon applying $S(\alpha, \beta)$ data. The differences can be seen at 0.05 - 0.1 eV $< E <$ 1 - 5 eV. Therefore, the inclusion of a proper $S(\alpha, \beta)$ data set for heavy water is necessary to obtain reliable estimates of k_{eff}. The impact of the

22

calculations with the CAB library is visible: the criticality decreased by 200 pcm (2 mk),

$$dk(\text{CAB}) =$$

$$k_{\text{eff}}(S(\alpha,\beta):\text{CAB}) - k_{\text{eff}}(S(\alpha,\beta):\text{ENDF/B-VII}) \approx$$

$$- 200 \text{ pcm}, \tag{11}$$

and the agreement between calculations and experimental results is improved with the CAB model. However, $|dk(\text{CAB})| < \delta k_{\text{bench}} \approx 330$ pcm.

An important assumption was made for the composition of NU uranium metal (fuel) and sheath (aluminum alloy 1-s) in the benchmark models: no impurities were taken into account, and this can introduce a bias into the results of modelling. To address the impact of impurities in the fuel rods, mass spectroscopy studies were performed in CNL, and the obtained fuel and sheath composition list was converted into the MCNP material cards (Atfield, 2014). The results of using the MCNP models with detailed material compositions are shown in Fig. 7. It was found that the impact of taken into account the impurities in the LEU-MET-THERM-003 models is a decrease in the criticality by ≈ 400 pcm $< 2\,\delta k_{\text{bench}}$, and the new results lie within the benchmark uncertainty. On the other hand, the impact of using CAB model for heavy water ($dk(\text{CAB})$) stays approximately the same as estimated in Eq. (11); compare Figs. 5 and 7.

Similar impact of changing from the ENDF/B-VII.0-based $S(\alpha,\beta)$ data for heavy water to the CAB model is found using another heavy water benchmark with NU metal rods arranged into a square lattice, tthe LEU-MET-THERM-001 benchmark (a critical assembly in the RB reactor, Belgrade, Serbia). We obtain

$$dk(\text{CAB}) \approx -260 \text{ pcm}, \tag{12}$$

and $|dk(\text{CAB})| < \delta k_{\text{bench}} = 570$ pcm. The results are shown in Fig. 7.

As reactor-grade heavy water was utilized in these benchmarks, it is important to estimate an impact on criticality originated from using $S(\alpha,\beta)$ data for H in H_2O for

23

modelling the neutron scattering on hydrogen (^{1}H) that is always present in the liquid D$_2$O. In Fig. 7, we present the results obtained by turning on and off the H-in-H$_2$O $S(\alpha,\beta)$ while the free gas model is used for other neutron scatterers present in heavy water. We found a noticeable change in criticality by $\simeq 100$ pcm for the LEU-MET-THERM-003 models, in which the heavy water has the purity of 99.3 - 99.4 wt.% D$_2$O. The impact of scattering on ^{1}H as H in H$_2$O is less significant for the LEU-MET-THERM-001 model, $dk(^1$H$) \simeq 10$ pcm, because the heavy water utilized in this benchmark is of a higher purity (99.82 wt.%).

Thus, applying the new evaluation for the scattering kernel of heavy water raises more questions on the nature of the biases observed in Figs. 5 and 7. For example, how does the accuracy of other cross sections in the ENDF/B-VII-based library impact the calculated criticality of LEU-MET-THERM-003? It is not clear whether there is a trend in the bias of k_{eff}(ENDF/B-VII) with the change of the lattice pitch. Therefore, more experimental results with the metal rod configurations have to be analyzed in detail (Altiparmakov, 2010).

4.2.2. ZED2-HWR-EXP-001

The ZED-2 critical cores described in the ZED2-HWR-EXP-001 benchmark (Atfield, 2015) consist of a hexagonal lattice of 55 fuel channels immersed in the heavy water that served as a moderator and reflector. The lattice pitch is 31 cm for all configurations included in this benchmark, and each fuel channel contained five vertically stacked fuel bundles. In turn, each fuel bundle is ≈ 50 cm long and contains a cluster of 28 fuel pins (natural uranium UO$_2$ in Zircaloy cladding).

The fuel channels, which are surrounded by heavy water moderator, are composed by two co-axial vertical pipes, an inner pipe called pressure tube (with the diameter of ≈ 10 cm and width of ≈ 0.3 cm) and an outer pipe called a calandria tube (with the diameter of ≈ 12.4 cm and width of ≈ 0.1 cm). The coolant is contained in the pressure tube, which are separated from the calandria tube by a gas annulus, and the calandria tubes are surrounded
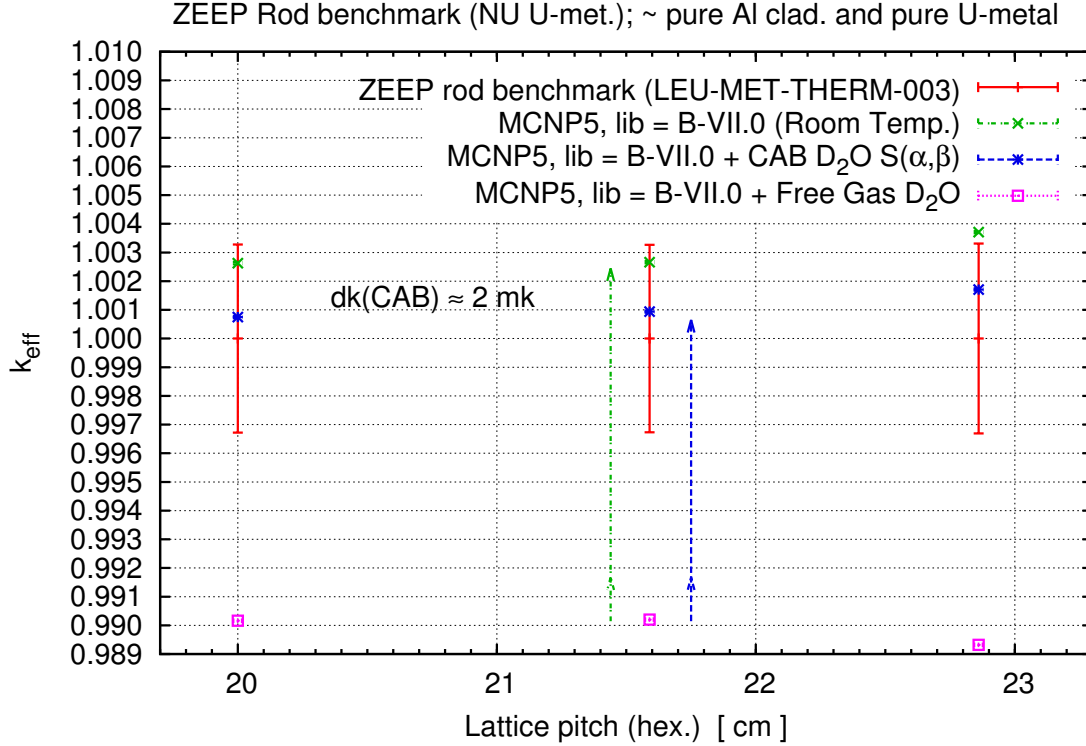
Figure 5: Experimental *vs.* computational results for the multiplication factor k_{eff} for the LEU-MET-THERM-003 benchmark as a function of the lattice pitch. (ZEEP rods are arranged into a hexagonal lattice.) The isotopic compositions of fuel (uranium metal) and sheath (aluminum alloy) were used without additional impurities. The impact of using the CAB model is that the criticality decreases by ≈ 200 pcm (2 mk) from the reference solution (ENDF/B-VII). The results obtained using the free gas model for D_2O are shown: free gas (FG) model introduces a large negative bias in k_{eff} (open pink squares). The arrows serve as an eye guide for changes in k_{eff} due to FG $\rightarrow S(\alpha,\beta)$.

by moderator. The fuel channels thus isolate the moderator from the coolant. Therefore, the coolant can be a different material (*e.g.*, air) and have a different temperature than the moderator (heavy water). For example, the case 1 of the ZED2-HWR-EXP-001 benchmark is a heavy-water moderated core with all channels being cooled by air. On the other hand, the case 8 is the heavy-water moderated core with all channels being cooled by heavy water. In the cases 2 to 7, a given number of the channels of the total 55 were cooled by the air and the rest is by the heavy water. For example, in the case 7, 37 channels of the total 55

25
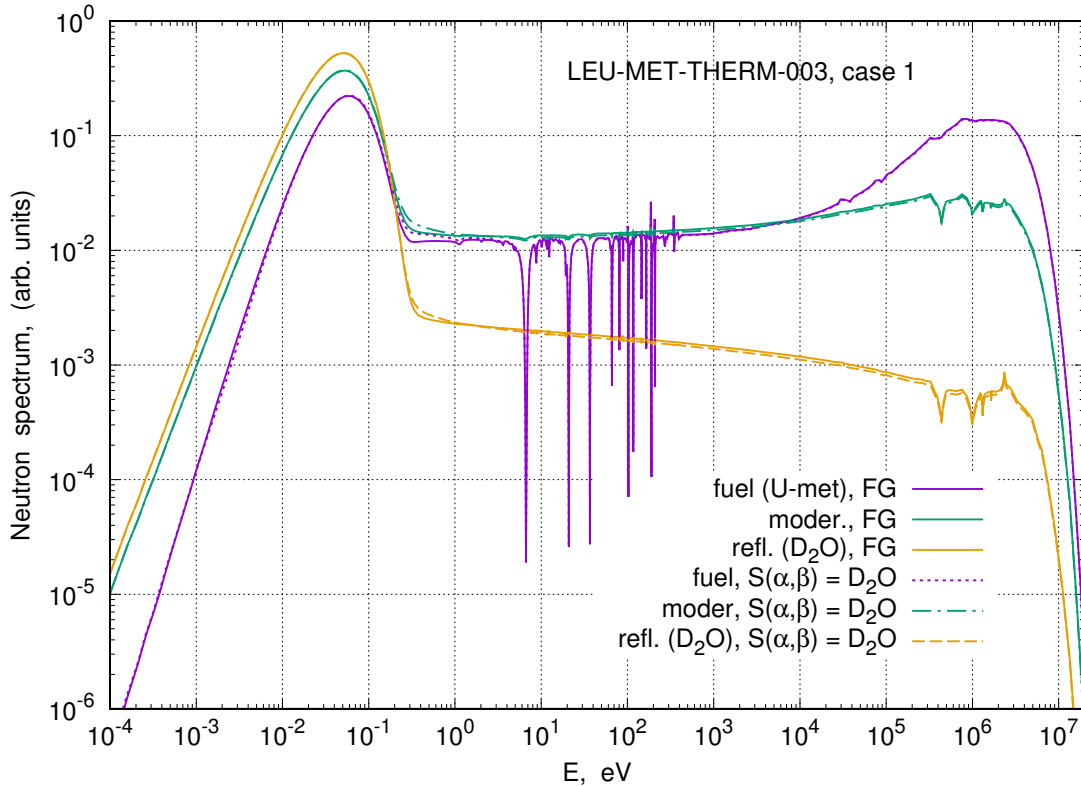
Figure 6: Neutron spectrum of the LEU-MET-THERM-003 benchmark (case 1, lattice pitch = 22.86 cm) in fuel (U metal), moderator, and reflector (D_2O). The results are obtained using free gas (FG) and CAB $S(\alpha, \beta)$ models for heavy water and MCNP6.1. Small changes in the spectra can be seen at 0.1 eV $< E <$ 1 - 4 eV upon FG $\rightarrow S(\alpha, \beta)$. The positions of maxima of the thermal peaks (at $2kT_{\mathrm{eff}} \simeq 0.05$ eV) and their widths are not changed significantly.

are cooled by D_2O and this will be marked as '(37/55 cooled)' in this study.

In channel type configurations, the $S(\alpha, \beta)$ data sets for the heavy water in the coolant and moderator have a different effect on the criticality. For example, assume we choose the free gas model for both the coolant and moderator and run all MCNP models that represent this benchmark. Then, the results have a visible negative bias in k_{eff} of ≈ 500 - 700 pcm ($k_{\mathrm{bench}} = 1.000 \pm 0.003$). To illustrate the subtle differences between the free gas model $vs.$ $S(\alpha, \beta)$ data for heavy water in the critical systems with thermal neutron spectrum ($e.g.$, the average neutron lethargy causing fission corresponds to $\simeq 0.1$ eV in ZED2-HWR-EXP-
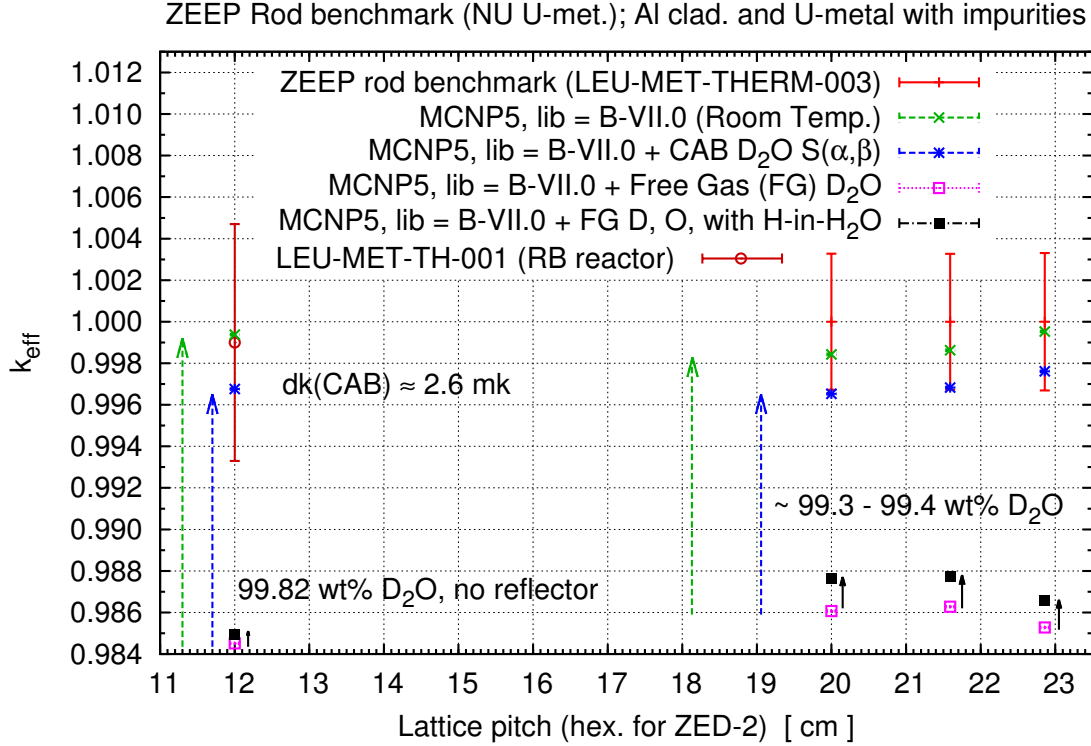
Figure 7: Experimental *vs.* computational results for the multiplication factor k_{eff} for the LEU-MET-THERM-003 benchmark. The isotopic compositions of the fuel (uranium metal) and sheath (aluminum alloy) include the impurities obtained by mass spectroscopy. For comparison, the results for the LEU-MET-THERM-001 benchmark are shown. The impact of using the CAB model is $\simeq 200$ pcm. The impact of $S(\alpha, \beta)$ data for ^{1}H in reactor-grade heavy water ($> 99\%$ of D_2O) is estimated by using the available TSL for H in liquid H_2O (black filled squares). The arrows serve as an eye guide for changes in k_{eff} due to $FG \to S_i(\alpha, \beta)$.

001), we show the neutron spectra in the fuel pins (UO_2), coolant and moderator (D_2O) in Fig. 8. The thermal peaks are slightly stronger and the lower part of the epi-thermal energy region (from $E > 0.1$ eV and up to $E \simeq 1$ eV) has a slightly larger neutron population with using $S(\alpha, \beta)$. If we apply the $S(\alpha, \beta)$ data for the heavy water in the moderator only, then the criticality goes up, similarly to the behaviour observed in modelling the critical cores of LEU-MET-THERM-003; compare Figs. 5 and 9. However, if we apply the $S(\alpha, \beta)$ data for heavy water in the coolant only, the criticality goes down by $\simeq 10$-100 pcm. Roughly, as
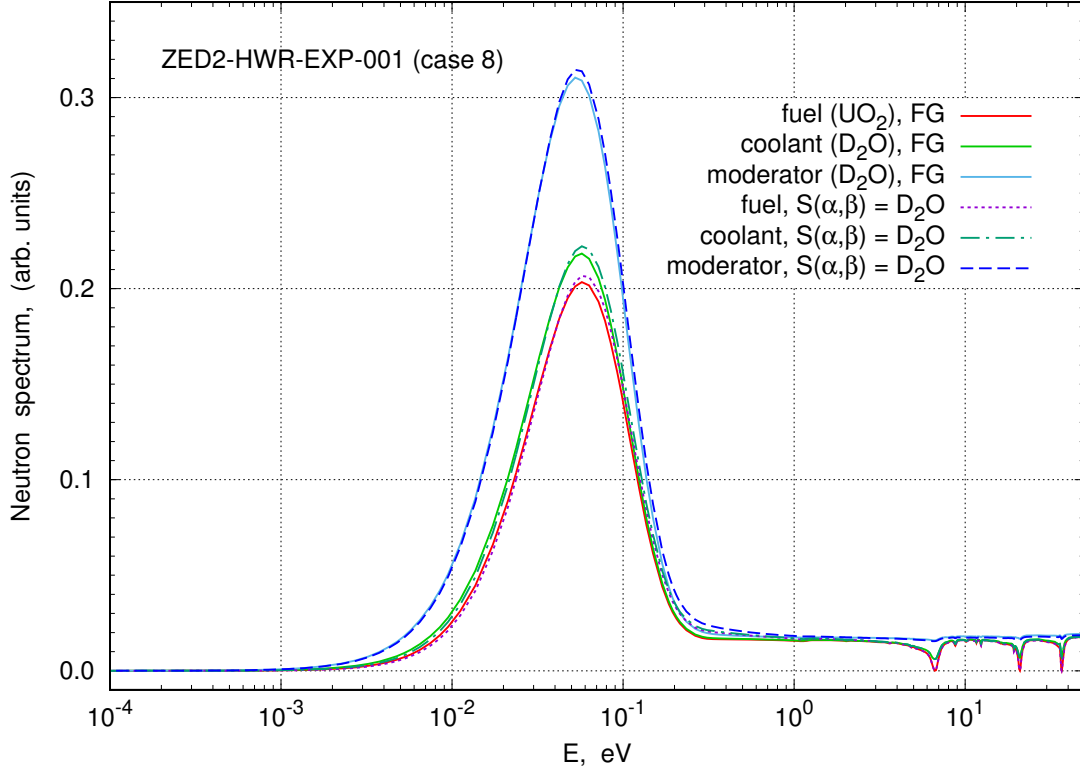
Figure 8: Neutron spectrum of the ZED2-HWR-EXP-001 benchmark (case 8, all channels cooled by D_2O) in fuel (UO_2), coolant, and moderator. The results are obtained using free gas (FG) and ENDF/B-VII $S(\alpha, \beta)$ models for heavy water and MCNP6.1. The thermal peaks are stronger with $S(\alpha, \beta)$, although the positions of maxima of thermal peaks (at $2kT_{\text{eff}} \simeq 0.05$ eV) and their widths are not changed significantly. Small changes in the neutron spectra are present at 0.1 eV $< E < 1$-4 eV.

the neutron up-scattering rate in the coolant is increased at 0.03-0.04 eV $< E < 5$-10 eV due to the $S(\alpha, \beta)$ treatment for heavy water, the neutron spectrum in the adjacent fuel pins gets harder. Then, the fission rate in UO_2 decreases while the capture rate increases, and k_{eff} goes down. The responses of k_{eff} against turning on the $S(\alpha, \beta)$ data in the different areas of the ZED-2 core are presented in Fig. 9. As the moderator and coolant purities are ≈ 99.82 wt.% D_2O in the ZED2-HWR-EXP-001 benchmark, the results of criticality turn out to be not sensitive to details of the scattering kernel (TSL) of ^{1}H that is present in the heavy water ($dk(^1\text{H}) \simeq 10$ pcm).
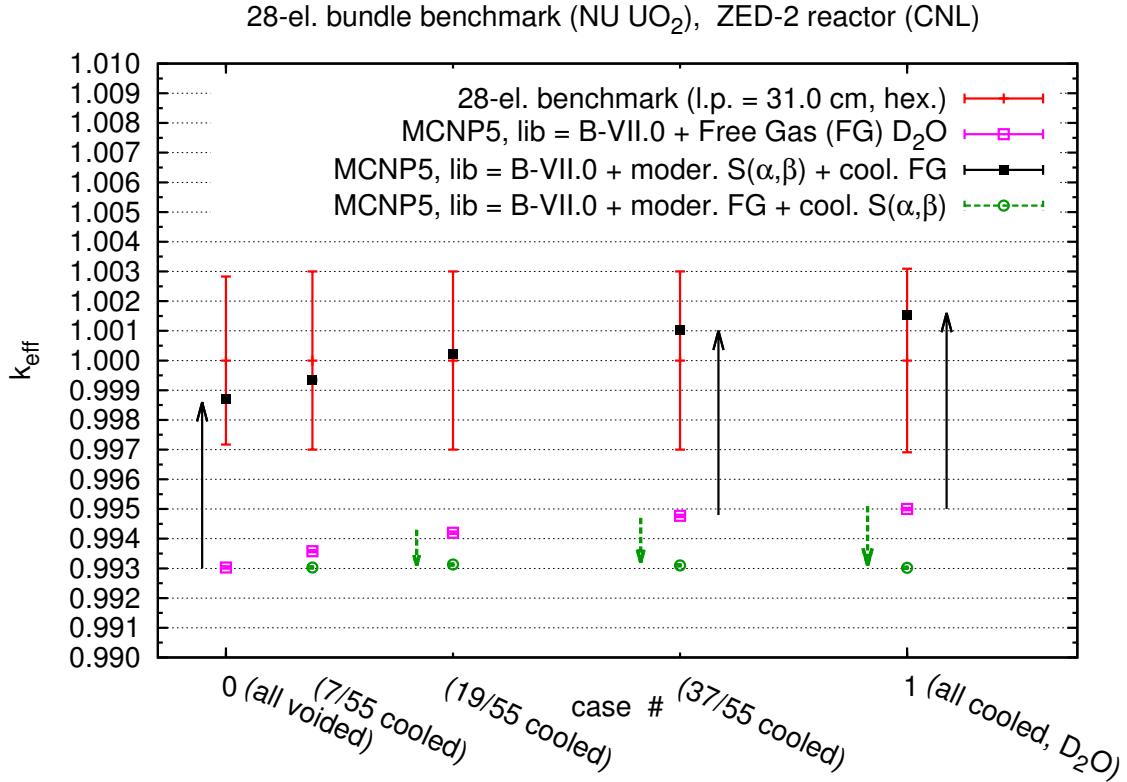
Figure 9: Experimental *vs.* computational results for the multiplication factor k_{eff} for the ZED2-HWR-EXP-001 benchmark. Using the free gas model for heavy water in these critical configurations, we obtains a negative bias in k_{eff} of ≈ 500-700 pcm (empty squares). Turning on the $S(\alpha, \beta)$ data in the moderator but not in the coolant results in increase of criticality (filled black squares). If the $S(\alpha, \beta)$ data is applied for the heavy water coolant but not for the moderator, criticality decreases in comparison with the fee gas results (open circles). The arrows serve as an eye guide for changes in k_{eff} due to FG $\rightarrow S(\alpha, \beta)$.

As a result of the different response to $S(\alpha, \beta)$ data between the moderator and coolant, there is a compensation effect in sensitivity of the ZED2-HWR-EXP-001 results to the change of $S(\alpha, \beta)$ data for heavy water. We obtain

$$dk(\text{CAB}) =$$
$$k_{\text{eff}}(S(\alpha, \beta) : \text{CAB}) - k_{\text{eff}}(S(\alpha, \beta) : \text{ENDF/B-VII}) \approx$$
$$- 100 \text{ pcm} \tag{13}$$

(or 1 mk), and $|dk(\mathrm{CAB})| < \delta k_{\mathrm{bench}} \approx 300\,\mathrm{pcm}$. The estimate of $dk(\mathrm{CAB})$ does not depend significantly on which configuration of the critical core the new data sets were applied to. The results for a few representative cores are shown in Fig. 10 ($k_{\mathrm{eff}}(\mathrm{CAB}) \approx 0.999$). We found that using either the ENDF/B-VII or CAB model for $S(\alpha, \beta)$ data for heavy water, the results of k_{eff} lie within the uncertainties of this critical benchmark. In addition, there is no significant trend in the bias of the calculated values of k_{eff} as the number of channels being cooled by the air was increased from 0, '(all cooled, D_2O)', to 55, '(all voided)'. It seems that the $S(\alpha, \beta)$ data in the D_2O coolant is responsible for such behaviour, $i.e.$, a constant bias in k_{eff} $vs.$ number of voided channels; compare Figs. 10 and 9.

4.2.3. CAB model with different evaluations for deuterium and oxygen

So far our analysis takes into consideration only the change of a single aspect in the microscopic nuclear data (the thermal scattering kernel of heavy water) in a complex calculation of the criticality of heterogeneous systems. However, modifying only one part of the microscopic cross sections might not necessarily lead to a visible improvement in the k_{eff} results, with discrepancies due to other imperfections of the nuclear data used in the calculations. In particular, some of the heavy water benchmarks show better agreement with experiments using older nuclear data libraries, which can be seen in the work by van der Marck (van der Marck, 2006) and Taylor and Hollenbach (Taylor and Hollenbach, 2013). For example, by substituting specific isotopes in the reference nuclear data library, it was found that the bias in HEU-SOL-THERM-004 and HEU-SOL-THERM-020 benchmarks is attributable to the deuterium evaluation in ENDF/B-VII.0 (= VII.1) (Taylor and Hollenbach, 2013; Kozier et al., 2011) in the epi-thermal energy region.

To analyze the behaviour of biases in k_{eff} observed in modelling the ZED-2 critical cores (LEU-MET-THERM-003 and ZED2-HWR-EXP-001), we replace the ENDF/B-VII evaluation of deuterium to other evaluations of $^2\mathrm{H}$ and run the same models using MCNP. Following Ref. (Márquez Damián et al., 2014a), we use the evaluation of deuterium included in the ROSFOND-2010 library (Zabrodskaya et al., 2007). The ROSFOND evaluation has a
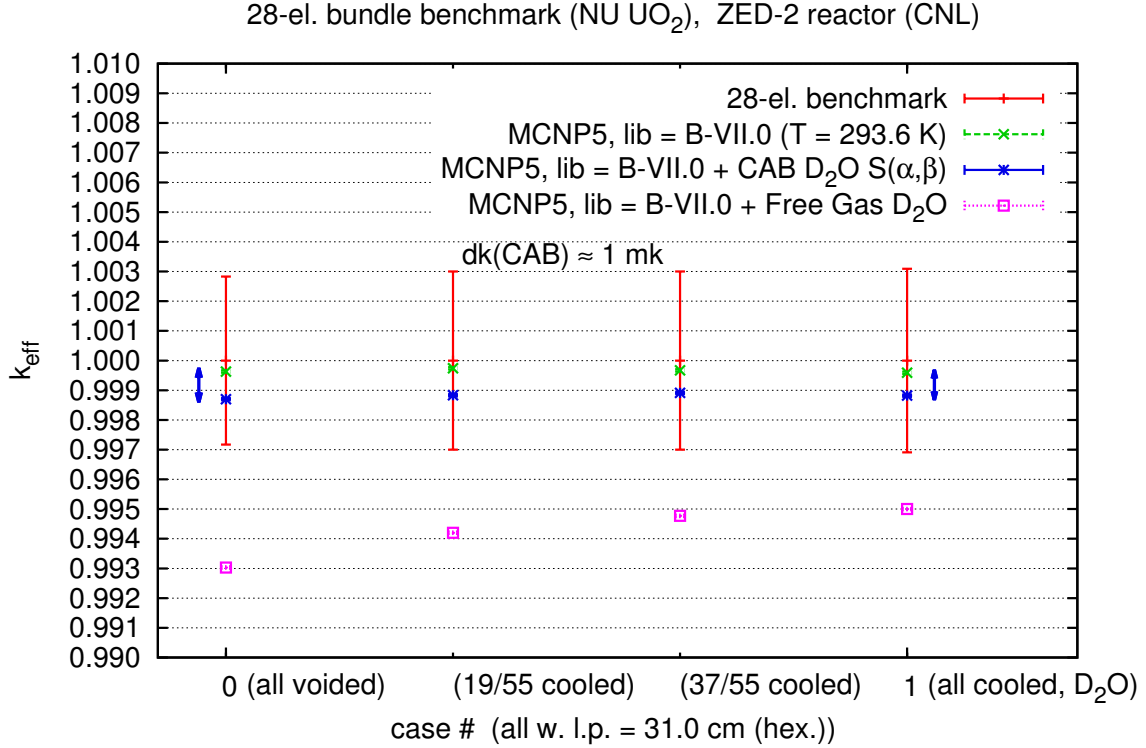
Figure 10: Experimental *vs.* computational results for the multiplication factor k_{eff} for selected critical cores from the ZED2-HWR-EXP-001 benchmark. The results obtained with the CAB and ENDF/B-VII models for $S(\alpha, \beta)$ data are shown. The impact of using the CAB model is the decrease of criticality by ≈ 100 pcm (1 mk) from the reference solution (ENDF/B-VII). The results obtained with free gas model are also shown for comparison (open squares).

slightly modified free atom scattering cross section ($\sigma_{\text{free}} = 3.390$ b against $\sigma_{\text{free}} = 3.395$ b in the ENDF/B-VII library, but the differences in the elastic neutron scattering are within the uncertainty of $\sigma_{\text{s, th}}(^2\text{H})$ ($\pm 0.35\%$ (Mughabghab, 2006)). There are also small differences in the neutron capture (*e.g.*, $\sigma_{\text{th}}(n, \gamma) = 0.519$ mb against 0.506 mb in the ENDF/B-VII library), and noticeable differences in the angular distributions of the elastic scattering at epi-thermal (fast) neutron energies (10 keV $< E < 3.2$ MeV).

It turns out that impact of the ROSFOND evaluation of ^2H on criticality of the LEU-MET-THERM-003 benchmark is not significant: although the changes in k_{eff} seem to
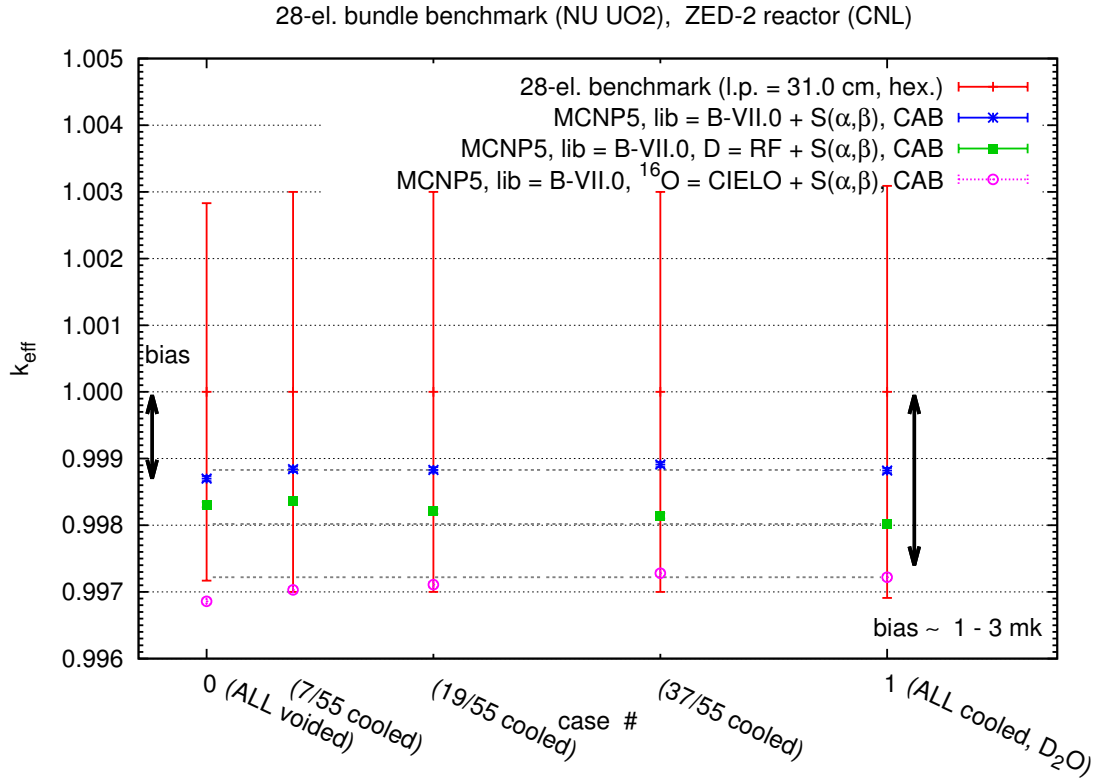
Figure 11: Experimental *vs.* computational results for the multiplication factor k_{eff} for selected critical cores from the ZED2-HWR-EXP-001 benchmark. The results are obtained using the CAB model for $S(\alpha, \beta)$ data (heavy water). The ENDF/B-VII evaluation of deuterium was changed to the ROSFOND-2010 (RF) one (filled squares used for the results), and the ENDF/B-VII evaluation of ^{16}O was changed to one of the CIELO evaluations for oxygen (results presented by open circles).

depend on the lattice pitch, they are ≤ 40 pcm; see Table 2. The impact is stronger for the ZED2-HWR-EXP-001 benchmark: the estimates of k_{eff} are decreased by $\lesssim 100$ pcm. The impact is strongest for the case with all channels being cooled by D_2O, and it is less for the configuration with all channels being voided; see Fig. 11. Yet all the results lie within the benchmark uncertainty, and we can conclude that, for the ZED-2 critical cores (LEU-MET-THERM-003 and ZED2-HWR-EXP-001), both the ENDF/B-VII.0 and ROSFOND-2010 evaluations of deuterium perform equally well with the CAB model for $S(\alpha, \beta)$. Similar results were obtained using the JEFF-3.2 evaluation of deuterium with

$\sigma_{\text{free}} = 3.382$ b (Morillon et al., 2013). For comparison, for the heavy water benchmarks analyzed in Ref. (Márquez Damián et al., 2014a), an improvement in the C/E ratio was obtained in 48 out of 65 cases by using the combination of ROSFOND ^{2}H and CAB $S(\alpha, \beta)$.

Deuterium (^{2}H) is the most important neutron scatterer in the thermal heavy water benchmarks, and the second in the list of scatterers is oxygen (^{16}O). As discussed in Ref. (Chadwick et al., 2014), the cross sections of ^{16}O(n,n) and ^{16}O(n,α) are biased in all modern evaluations of ^{16}O, and the new trial evaluations of ^{16}O were proposed within the CIELO project (WPEC Subgroup 40 (Chadwick et al., 2014; WPEC Subgroup 40, 2013)) in attempt to improve the description of (n,n), (n,α) and other reaction channels of $n + {}^{16}$O. In the thermal systems with UO$_2$ fuel and heavy water, the impact of changes in the neutron capture due to ^{16}O(n,α) in the fuel elements and coolant/moderator is expected to be of less importance for the estimates of criticality. In the thermal systems, ^{16}O is one of the important neutron scatterers, with the flux averaged cross section $\langle\sigma_s(^{16}\text{O})\rangle \simeq 3.7$ b. Use of the new trial evaluations of ^{16}O in modelling the thermal critical systems is expected to aid in the assessing the impact of a decrease in $\langle\sigma_s(^{16}\text{O})\rangle$ (and $\langle\sigma_{\text{tot}}(^{16}\text{O})\rangle$) by $\simeq 1\text{-}2\%$. It is expected that the criticality will decrease as well (Roubtsov et al., 2014; Leal et al., 2016).

To analyze the impact of ^{16}O cross sections on k_{eff} of the ZED-2 critical cores (LEU-MET-THERM-003 and ZED2-HWR-EXP-001), we replaced the ENDF/B-VII evaluation of ^{16}O to one of the CIELO trail evaluations and renormalized the CAB model to the corresponding $\sigma_{\text{free}}(^{16}\text{O}) = 3.794$ b [3]. Then the criticality (k_{eff}) of the ZED-2 reactor cores is further decreased by $\approx 100\text{-}200$ pcm ($1\text{-}2$ mk); see Table 2 and Fig. 11. Using the CAB model for $S(\alpha, \beta)$ and CIELO evaluation for ^{16}O, we found that the results for the LEU-MET-THERM-003 benchmark are, roughly, $k_{\text{eff}} \approx 0.996$ (models with impurities), *i.e.*, they are negatively biased and fall outside of $k_{\text{bench}} - \delta k_{\text{bench}} \approx 0.997$. The impact of the new evaluation of ^{16}O is stronger for the LEU-MET-THERM-001. However, δk_{bench}

---

[3]The CIELO evaluation of ^{16}O used in this study is `O16e80b1`; see `https://www-nds.iaea.org/CIELO/`.

is larger (570 pcm), and the new estimate, $k_{\text{eff}} \approx 0.995$, stays within the benchmark uncertainty $k_{\text{bench}} \pm \delta k_{\text{bench}}$.

For the ZED2-HWR-EXP-001 benchmark, the new ^{16}O (CIELO) evaluation and CAB model for $S(\alpha, \beta)$ result in the decrease of k_{eff} by $\simeq$ 160-170 pcm. We obtain, roughly, $k_{\text{eff}} \approx 0.997$, *i.e.*, the new estimates of k_{eff} are negatively biased by ≈ 300 pcm. Moreover, for the fully voided configuration, the estimate of k_{eff} lies slightly out of $k_{\text{bench}} - \delta k_{\text{bench}}$; see Fig. 11. We notice that, with the benchmark uncertainty of $\approx \pm 300$ pcm and the obtained results biased by $\simeq$ 100-300 pcm, any minor additional bias in the estimate of criticality due to a possible trend in k_{eff} with an increase number of air-cooled channels cannot be revealed rigorously in this study. In addition, based on the assumptions made in building the representative MCNP models of the ZED-2 benchmarks (Chow, 2012) as well as the approximations and cut-offs used in the algorithms of MCNP itself (Becker et al., 2009), it would not be appropriate to claim that the accuracy of the presented results (MCNP models) is better than ± 10 pcm.

It is natural to expect that the estimates of criticality of the ZED-2 cores loaded with the natural uranium fuel are sensitive to the evaluations of the neutron cross sections of uranium, and the CIELO project provides the new evaluations of ^{235}U and ^{238}U for testing. It turns out that substitution of the ENDF/B-VII.0 evaluations of ^{235}U and ^{238}U for the CIELO evaluations u235_CIELO20170217 and u238_CIELO20170215 improves the estimates of k_{eff}. For example, using the CAB models for heavy water TSL and the CIELO evaluations for ^{16}O, ^{235}U, and ^{238}U, we obtain $k_{\text{eff}} \approx 0.9965$-0.9968 for LEU-MET-THERM-003 and $k_{\text{eff}} \approx 0.998$ for ZED2-HWR-EXP-001; see the last column of Table 2. The effect of the new CIELO evaluations of ^{235}U and ^{238}U can be attributed mainly to the decrease in ^{238}U(n,g) reaction rate in the resonance energy region. The impact is stronger for the ZED2-HWR-EXP-001 benchmark: the difference in k_{eff} is ≈ 100 pcm, and the averaged capture cross sections of ^{238}U in the fuel elements ($\langle \sigma(^{238}\text{U}(n,g)) \rangle \simeq 1$ b) are different by $\approx 0.4\%$.

Thus, the results presented here demonstrate that applying improved nuclear data sets for selected critical benchmarks with accurate estimates of the benchmark uncertainties, such as, $k_{\mathrm{bench}}(\text{ZED-2}) \approx 1.000 \pm 0.003$, could reveal the biases in k_{eff} undetected so far by modelling with only the reference evaluated nuclear data library (such as, *e.g.*, ENDF/B-VII.0). Therefore, additional studies of these benchmarks with different versions of the evaluated nuclear data libraries could be of interest.

Table 2: Benchmark and computed multiplication factors for selected heavy water critical systems.
The LEU-MET-THERM-003 models without impurities in U metal and Al cladding are marked by (p), and the cases with impurities in these materials are marked by (i). In the ZED2-HWR-EXP-001 benchmark, case 1 corresponds to the fully voided core (all channels cooled by air), and case 8 corresponds to the fully cooled one (all channels cooled by D_2O). ENDF/B-VII.0 is used for the reference estimates of k_{eff}; ROSFOND-2010 and CIELO evaluations are shortened to RF-2010 and CL.

Benchmark with case ID	Benchmark k_{eff}	ENDF/B-VII k_{eff}	CAB Model (B-VII ^{2}H, ^{16}O)	CAB Model $+$ RF-2010 ^{2}H	CAB Model $+$ CL ^{16}O	CAB Model $+$ CL ^{16}O,^{5,8}U
LEU-MET-THERM-001-1	0.99900(570)	0.99938(4)	0.99676(4)	0.99752(4)	0.99461(4)	0.99574(4)
LEU-MET-THERM-003-1(p)	1.00000(331)	1.00371(4)	1.00171(4)	1.00130(4)	0.99994(4)	1.00064(4)
LEU-MET-THERM-003-2(p)	1.00000(327)	1.00266(4)	1.00094(4)	1.00066(4)	0.99991(4)	1.00070(4)
LEU-MET-THERM-003-3(p)	1.00000(328)	1.00263(4)	1.00075(4)	1.00060(4)	1.00012(4)	1.00089(4)
LEU-MET-THERM-003-1(i)	1.00000(331)	0.99953(4)	0.99761(4)	0.99725(4)	0.99582(4)	0.99653(4)
LEU-MET-THERM-003-2(i)	1.00000(327)	0.99863(4)	0.99683(4)	0.99664(4)	0.99573(4)	0.99657(4)
LEU-MET-THERM-003-3(i)	1.00000(328)	0.99843(4)	0.99653(4)	0.99656(4)	0.99606(4)	0.99680(4)
ZED2-HWR-EXP-001-1	1.00000(283)	0.99963(4)	0.99870(4)	0.99831(4)	0.99686(4)	0.99788(4)
ZED2-HWR-EXP-001-2	1.00000(283)	0.99968(4)	0.99864(4)	0.99830(4)	0.99687(4)	0.99812(4)
ZED2-HWR-EXP-001-3	1.00000(283)	0.99976(4)	0.99875(4)	0.99839(4)	0.99687(4)	0.99850(4)
ZED2-HWR-EXP-001-4	1.00000(300)	0.99975(4)	0.99874(4)	0.99834(4)	0.99699(4)	0.99790(4)
ZED2-HWR-EXP-001-5	1.00000(300)	0.99978(4)	0.99884(4)	0.99837(4)	0.99703(4)	0.99806(4)
ZED2-HWR-EXP-001-6	1.00000(300)	0.99974(4)	0.99883(4)	0.99821(4)	0.99711(4)	0.99812(4)
ZED2-HWR-EXP-001-7	1.00000(300)	0.99967(4)	0.99891(4)	0.99814(4)	0.99728(4)	0.99820(4)
ZED2-HWR-EXP-001-8	1.00000(309)	0.99959(4)	0.99882(4)	0.99802(4)	0.99722(4)	0.99834(4)

36

5. Summary and Conclusions

The CAB thermal scattering law for heavy water represent an improvement over existing TSLs available in the modern evaluated nuclear data libraries from the standpoint of better agreement with microscopic data. Some improvement was found in the cold neutron energy range, which has little impact on the thermal critical systems, but other improvements – related to a better representation of the neutron scattering in oxygen – are in the thermal energy region where the accurate description of neutron spectrum is important for the heavy water moderated systems. In particular, the re-evaluated total cross sections of heavy water show very good agreement with the available experimental data at room temperature (Márquez Damián et al., 2015), and all the features of experimental data *vs.* incident neutron energy are reproduced well by the CAB model. The calculated average scattering cosine (μ-bar) of heavy water follows the available experimental data, and very good agreement was found. The effective temperature of deuterium and oxygen in heavy water were re-evaluated using the CAB model, and the new estimates agree well with the experimental results obtained using deep inelastic neutron scattering technique (Dawidowski et al., 2016). As the CAB models for the thermal scattering kernels are given in ENDF-6 format (file MF7), the data files can be converted to application-specific library files and be used with reference level codes, such as MCNP. Moreover, the new evaluations for heavy and light water based on the CAB models can be made consistent with any modern evaluated nuclear data library. In this study, we use ENDF/B-VII.0 as the reference nuclear data library in our modelling with MCNP5.

The new thermal scattering libraries for heavy water were applied to the calculation of neutron criticality benchmarks, and improvements were found in the calculation in 60% of relevant thermal systems (Márquez Damián et al., 2014a). However, in the previous studies, the critical cores of the ZED-2 reactor were not analyzed in detail from the standpoint of application of the $S(\alpha, \beta)$ data; a more detailed analysis has been presented here. The estimates of k_{eff} of the ZED-2 critical cores were obtained with the ENDF/B-VII $S(\alpha, \beta)$

37

data for heavy water and compared for the same model, code, and nuclear data file with one exception: the CAB model were applied for the heavy water $S(\alpha, \beta)$ data, *i.e.*, for the isotopes of deuterium, oxygen (^{16}O), and hydrogen (^{1}H). As a result, k_{eff}(ZED-2) decreases by $\simeq 100\text{-}200$ pcm.

The models of LEU-MET-THERM-003 benchmark show better agreement with the experiments ($k_{\mathrm{bench}} = 1.0$) with the CAB model for $S(\alpha, \beta)$ if the simplified models (without impurities in the fuel and sheath) were used to obtain the estimates of k_{eff}. However, the impurities has a stronger impact on criticality than the changes in $S(\alpha, \beta)$ model for heavy water. Then, the combined effect of impurities in the fuel rods and the CAB $S(\alpha, \beta)$ data for heavy water results in the estimates of k_{eff} still lying within the benchmark uncertainty, with a negative bias in k_{eff} of ≈ 300 pcm. Moreover, changing the basic nuclear data file for ^{16}O to a new and improved evaluation from the CIELO project (Chadwick et al., 2014) drives the criticality of LEU-MET-THERM-003 down by adding up to 100 pcm to the bias in k_{eff}. Application of the CIELO evaluations for ^{235}U and ^{238}U improves the estimates of k_{eff}, but the negative bias of $\simeq 350$ pcm is still visible. Thus, these results indicate the need for additional studies of the criticality of simple benchmarks with uranium metal rods in heavy water.

We found that, using the models of ZED2-HWR-EXP-001 benchmark, one cannot differentiate between the ENDF/B-VII $S(\alpha, \beta)$ data and the CAB model for heavy water because the results obtained with MCNP lie within $k_{\mathrm{bench}} \pm \delta k_{\mathrm{bench}}$. The results obtained with the CAB model are biased by ≈ 100 pcm from $k_{\mathrm{bench}} = 1.0$, and the bias stays constant (within $\approx \pm 10$ pcm). This means that the bias in k_{eff} is independent of the configuration of the critical cores included into the ZED2-HWR-EXP-001 benchmark to test the voiding effect (coolant $D_2O \rightarrow$ air at room temperature). To test the sensitivity of the bias in k_{eff} to changes in the basic nuclear data files for deuterium and oxygen, we substituted the ENDF/B-VII.0 data files with the ROSFOND-2010 (for ^{2}H) and CIELO project (for ^{16}O) and re-ran the benchmark models. From our observations it was concluded that the

effect of the ROSFOND-2010 ^{2}H is not significant: the changes in k_{eff} are $\lesssim 100$ pcm. On the other hand, the new CIELO evaluations of ^{16}O have a stronger impact: the estimated criticality of ZED2-HWR-EXP-001 decreases by ≈ 100 - 200 pcm, and the combined effect of the CAB model for $S(\alpha, \beta)$ and the CIELO evaluation of ^{16}O results in a negative bias of k_{eff} of ≈ 300 pcm, which is almost equal to δk_{bench}. However, application of the CIELO evaluations for ^{235}U and ^{238}U improves the estimates of k_{eff}, but the negative bias of $\simeq 200$ pcm is still visible. Therefore, additional studies of this benchmark with different nuclear data options would be of interest, such as, for example, using the ENDF/B-VIII.0 and JEFF-3.3 evaluations that are currently under the beta testing stage.

References

Altiparmakov, D., 2010. ENDF/B-VII.0 versus ENDF/B-VI.8 in CANDU$^{©}$ Calculations. In: Proceedings of PHYSOR 2010 – Advances in Reactor Physics to Power the Nuclear Renaissance, Pittsburgh, Pennsylvania, USA. American Nuclear Society, LaGrange Park, IL, USA, (on CD ROM).

Atfield, J., 2014. private communication.

Atfield, J., 2015. 28-element natural UO_2 fuel assemblies in ZED-2 (ZED2-HWR-EXP-001). In: Bess, J. (Ed.), International Handbook of Evaluated Reactor Physics Benchmark Experiments (IRPhEP). OECD Nuclear Energy Agency, Paris.

Atfield, J., 2016. ZED-2 reactor: Natural-uranium metal fuel assemblies in heavy-water (LEU-MET-THERM-003). In: Briggs, J. (Ed.), International Handbook of Evaluated Criticality Safety Benchmark Experiments (ICSBEP). OECD Nuclear Energy Agency, Paris.

Bayly, J., Kartha, V., Stevens, W., 1963. The absorption spectra of liquid phase H_2O, HDO and D_2O from 0.7 μm to 10μm. Infrared Physics 3, 211–223.

Becker, B., Dagan, R., Lohnert, G., 2009. Proof and implementation of the stochastic formula for ideal gas, energy dependent scattering kernel. Annals of Nuclear Energy 36, 470–474.

Bée, M., 1988. Quasielatic Neutron Scattering. Principles and Applications in Solid State Chemistry, Biology, and Material Science. Adam Hilger, Bristol and Philadelphia.

Bess, J. (Ed.), 2015. International Handbook of Evaluated Reactor Physics Benchmark Experiments (IRPhEP). OECD Nuclear Energy Agency, Paris, NEA/NSC/DOC(2006)01.

Beyster, J., Antunez, H., Brouwer, W., Carriveau, G., Crosbie, K., Koppel, J., Naliboff,

Y., Neill, J., Russell Jr., J., Young, J., Young, J., 1965. Integral neutron thermalization. Annual Summary Report GA-6824, General Atomics Technical Report.

Briggs, J. (Ed.), 2016. International Handbook of Evaluated Criticality Safety Benchmark Experiments (ICSBEP). OECD Nuclear Energy Agency, Paris, NEA/NSC/DOC(95)03.

Chadwick, M., Dupont, E., et al., 2014. The CIELO Collaboration: Neutron Reactions on ^{1}H, ^{16}O, ^{56}Fe, ^{235,238}U, and ^{239}Pu. Nuclear Data Sheets 118, 1–25.

Chadwick, M., Herman, M., Obložinskỳ, P., Dunn, M. E., Danon, Y., Kahler, A., Smith, D. L., Pritychenko, B., Arbanas, G., Arcilla, R., et al., 2011. ENDF/B-VII.1 nuclear data for science and technology: Cross sections, covariances, fission product yields and decay data. Nuclear Data Sheets 112 (12), 2887–2996.

Chadwick, M., Obložinskỳ, P., Herman, M., Greene, N., et al., 2006. ENDF/B-VII.0: next generation evaluated nuclear data library for nuclear science and technology. Nuclear Data Sheets 107 (12), 2931–3060.

Chow, J., 2012. The Development of Model Generators for Specific Reactors. In: Proceedings of 24$^{\text{th}}$ Nuclear Simulation Symposium, Ottawa, Ontario, Canada. Canadian Nuclear Society, (on CD ROM).

Dawidowski, J., Rodríguez Palomino, L., Márquez Damián, J., Blostein, J., Cuello, G., 2016. Effective temperatures and scattering cross sections in water mixtures determined by Deep Inelastic Neutron Scattering. Annals of Nuclear Energy 90, 247–255.

Edura, Y., Morishima, N., 2005. Cold and thermal neutron scattering in liquid water-II: scattering laws and group constants for H_2O and D_2O. Nucl. Instr. and Methods-A 545, 309–318.

Edura, Y., Morishima, N., 2006. Generation of neutron multigroup constants in the energy

range 0.1 μeV–10 MeV for light and heavy water at four different temperatures. Nucl. Instr. and Methods-A 560, 485–493.

Farhi, E., Ferran, G., Haeck, W., Pellegrini, E., Calzavara, Y., 2015. Light and heavy water dynamic structure factor for neutron transport codes. Journal of Nuclear Science and Technology 52 (6), 844–856.

González, M., Abascal, J., 2011. A flexible model for water based on TIP4P/2005. The Journal of Chemical Physics 135 (22), 224516–224516.

Goorley, T., James, M., Booth, T., Brown, F., Bull, J., Cox, L., Durkee, J., et al., 2012. Initial MCNP6 release overview. Nuclear Technology 180 (3), 298–315.

Gray, J., Guest, A., 1986. ^{17}O and ^{18}O analysis of heavy water. Applied Radiation and Isotopes 37 (9), 969–971.

Haywood, B., 1967. The spectral density of hydrogen in water. Journal of Nuclear Energy 21, 249–262.

Henry, A., 1975. Nuclear-reactor analysis. MIT Press Cambridge, (MA).

Kahler, A., MacFarlane, R., Mosteller, R., Kiedrowski, B., Frankle, S., Chadwick, M., McKnight, R., Lell, R., Palmiotti, G., Hiruta, H., et al., 2011. ENDF/B-VII.1 neutron cross section data testing with critical assembly benchmarks and reactor experiments. Nuclear Data Sheets 112 (12), 2997–3036.

Keinert, J., Mattes, M., Sartori, E., 1984. JEF-1 scattering law data. Tech. Rep. JEF Report 2, JEF/DOC 41.2, IKE 6-147, IKE Stuttgart.

Kim, J., Park, Y., Song, K., 2011. Analysis of the HDO content in heavy water by ATR-FTIR. Journal of Radioanalytical and Nuclear Chemistry 287, 723–728.

Koppel, J., Houston, D., 1978. Reference manual for ENDF thermal neutron scattering data. Tech. Rep. GA-8774 REVISED, ENDF-269, Gulf General Atomics, USA.

Kornbichler, S., 1965. Determination of the diffusion constants $D(E,T)$ and $D(T)$ of thermal neutrons in H_2O, phenylene, $ZrH_{1.92}$, and D_2O by measurement of scattering angular distributions. II. Zirconium hydride and heavy water. Nukleonik 7, 281–286.

Kozier, K., Roubtsov, D., Plompen, A., Kopecky, S., 2013. Reactivity impact of ^{16}O thermal elastic-scattering nuclear data for some numerical and critical benchmark systems. Nuclear Technology 183, 473–483.

Kozier, K., Roubtsov, D., Rao, R., Svenne, J., Canton, L., Plompen, A., Stanoiu, M., Nankov, M., Rouki, C., 2011. Status of deuterium nuclear data for simulation of heavy water reactors. In: Proceedings of International Conference on Future of Heavy Water Reactors, Ottawa, Ontario, Canada, October 02-05. CNS, Canada, paper 054, on CD-ROM.

Kropff, F., Latorre, J., Granada, J., Madero, C. C., 1974. Total neutron cross-section of D2O at 20 degrees-C between 0.0005 and 10 eV, EXFOR # 30283002. `https://www-nds.iaea.org/exfor/exfor.htm`.

Leal, L., Ivanov, E., Noguere, G., Plompen, A., Kopecky, S., 2016. Resonance parameter and covariance evaluation for ^{16}O up to 6 MeV. EPJ Nuclear Sci. Technol. 2, 43.

Lewis, E., Miller Jr., W., 1993. Computational methods of neutron transport. American Nuclear Society, La Grange Park, (IL).

Li, G., Bentoumi, G., Tun, Z., Li, L., Sur, B., 2017. Thermal neutron scattering cross-section measurements of heavy water. CNL Nuclear Review 6 (1), 47–53.

Lisichkin, Y., Saharova, L., Marti, J., Novikov, A., 2005. Temperature dependence of the generalized frequency distribution of water molecules: comparison of experiments and molecular dynamics simulations. Molecular Simulation 31 (14), 1019–1025.

Lovesey, S., 1984. Theory of neutron scattering from condensed matter. Vol. 1. Clarendon Press Oxford.

MacFarlane, R., 1994. New thermal neutron scattering files for ENDF/B-VI release 2. Tech. Rep. LA-12639-MS (ENDF 356), Los Alamos National Laboratory, USA.

MacFarlane, R., 2010. Neutron slowing down and thermalization. In: Cacuci, D. (Ed.), Handbook of Nuclear Engeneering, Vol. 1. Springer, pp. 188–277.

MacFarlane, R., Kahler, A., 2010. Methods of processing ENDF/B-VII with NJOY. Nuclear Data Sheets 111, 2739–2890.

MacFarlane, R., Muir, D., 1999. The NJOY Nuclear Data Processing System, Version 99. Tech. rep., Los Alamos National Laboratory, USA, `http://t2.lanl.gov/nis/codes.shtml`.

Márquez Damián, J., Granada, J., Baxter, D., Parnell, S., Evans, D., 2015. Measurement of the total cross section of heavy water in the 0.1 meV–1 eV energy range at 20 and 50 °C. Nuovo Cimento C 38, 178.

Márquez Damián, J., Granada, J., Roubtsov, D., 2014a. Improvement on the calculation of D_2O moderated critical systems with new thermal neutron scattering libraries. Annals of Nuclear Energy 71, 206–210.

Márquez Damián, J. I., Malaspina, D., Granada, J., 2013. Vibrational spectra of light and heavy water with application to neutron cross section calculations. The Journal of Chemical Physics 139 (2), 024504.

Márquez Damián, J. I., Malaspina, D., Granada, J. R., 2014b. CAB Models for Water: A New Evaluation of the Thermal Neutron Scattering Laws for Light and Heavy Water in ENDF-6 format. Annals of Nuclear Energy 65, 280–289.

Marti, J., Padro, J., Guardia, E., 1996. Molecular dynamics simulation of liquid water along the coexistence curve: Hydrogen bonds and vibrational spectra. The Journal of Chemical Physics 105, 639.

Mattes, M., Keinert, J., 2005. Thermal neutron scattering data for the moderator materials H_2O, D_2O and ZrH_x in ENDF-6 format and as ACE library for MCNP(X) codes. Tech. Rep. INDC(NDS)-0470, IAEA, Vienna.

Morillon, B., Lazauskas, R., Carbonell, J., 2013. Influence of the *ab initio* n–d cross sections in the critical heavy-water benchmarks. Annals of Nuclear Energy 54, 167–177.

Morishima, N., 2006. CLES: cross section library of moderator materials for low-energy neutron sources. RSICC Data Package DLC-233, `https://rsicc.ornl.gov/Default.aspx`.

Morishima, N., Aoki, Y., 1995. Evaluation of cold neutron scattering cross sections for light and heavy water. Annals of Nuclear Energy 22 (3-4), 147–158.

Mughabghab, S., 2006. Atlas of neutron resonances. Elsevier Science.

Roubtsov, D., 2015. Nuclear Data Testing and Evaluation at CNL (Canada) and CAB (Argentina). Presentation, CSEWG Annual Meeting, USA.

Roubtsov, D., Kozier, K., Chow, J., Plompen, A., Kopecky, S., Svenne, J., Canton, L., 2014. Reactivity impact of ^{2}H and ^{16}O elastic scattering nuclear data on critical systems with heavy water. Nuclear Data Sheets 118, 414–417.

Sinitsa, V., Rineiskij, A., 1993. GRUCON - A Package of Applied Computer Programs System Input and Operating Procedures of Functional Modules. Report INDC-CCP-0344, International Atomic Energy Agency, Vienna, Austria.

Sköld, K., 1967. Small energy transfer scattering of cold neutrons from liquid argon. Physical Review Letters 19 (18), 1023–1025.

Soper, A., 2013. The Radial Distribution Functions of Water as Derived from Radiation Total Scattering Experiments: Is There Anything We Can Say for Sure? ISRN Physical Chemistry 2013, 1–67, Article ID 279463.

Soper, A., Benmore, C., 2008. Quantum differences between heavy and light water. Physical Review Letters 101 (6), 065502.

Taylor, R., Hollenbach, D., June 2013. Variations in Computed Neutron Multiplication of Deuterium Moderated Highly Enriched Uranium Systems. Trans. Am. Nuclear Soc. 108, 509.

Trkov, A., Herman, M., Brown, D., 2011. ENDF-6 formats manual. Tech. Rep. Report BNL-90365-2009 Rev. 2, Brookhaven National Laboratory, USA.

USNDP/CSEWG GForge Collaboration Server, 2017. ENDF/A Thermal Scattering Sub-library. `https://ndclx4.bnl.gov/gf/project/endf/scmsvn/?action=browse&path=/trunk/endf7/thermal_scatt/`.

van der Marck, S., 2006. Benchmarking ENDF/B-VII.0. Nuclear Data Sheets 107 (12), 3061–3118.

van der Marck, S., 2012. Benchmarking ENDF/B-VII.1, JENDL-4.0 and JEFF-3.1.1 with MCNP6. Nuclear Data Sheets 113 (12), 2935–3005.

Van Der Spoel, D., Lindahl, E., Hess, B., Groenhof, G., Mark, A., Berendsen, H., 2005. GROMACS: fast, flexible, and free. Journal of Computational Chemistry 26 (16), 1701–1718.

Vineyard, G., 1958. Scattering of slow neutrons by a liquid. Physical Review 110 (5), 999–1010.

Williams, M., 1966. The slowing down and thermalization of neutrons. North-Holland Publishing Company, Amsterdam, Netherlands.

WPEC Subgroup 40, 2013. Collaborative International Evaluated Library Organisation Pilot Project (CIELO). `https://www.oecd-nea.org/science/wpec/sg40-cielo/`.

X-5 Monte Carlo Team, Brown, F., 2005. MCNP – a general Monte Carlo N-particle transport code, version 5. Tech. Rep. LA-UR-03-1987 (Revised), Los Alamos National Laboratory, USA.

Zabrodskaya, S., Ignatyuk, A., Kosheev, V., Nikolaev, M., Pronyaev, V., 2007. ROSFOND – Russian National Library of Neutron Data. VANT (Voprosi Atomnoy Nauki i Techniki) Ser. Nuclear Constants 1–2, 3–21.